Metallogeny of the Baiyangping Lead-Zinc Polymetallic Ore Concentration Area, Northern Lanping Basin of Yunnan Province, China

WANG Xiaohu[1, 2, *], SONG Yucai[3], ZHANG Hongrui[3], LIU Yingchao[3], PAN Xiaofei[3] and GUO Tao[2]

1 *China University of Geosciences, Beijing 100083, China*
2 *Laboratory of Dynamic Diagenesis and Metallogenesis, Institute of Geomechanics, Chinese Academy of Geological Sciences, Beijing 100081, China*
3 *Institute of Geology, Chinese Academy of Geological Sciences, Beijing 100037, China*

Abstract: The Lanping Basin in the Nujiang-Lancangjiang-Jinshajiang (the Sanjiang) area of northeastern margin of the Tibetan Plateau is an important part of eastern Tethyan metallogenic domain. This basin hosts a number of large unique sediment-hosted Pb-Zn polymetallic deposits or ore districts, such as the Baiyangping ore concentration area which is one of the representative ore district. The Baiyangping ore concentration area can be divided into the east and west ore belts, which were formed in a folded tectogene of the India-Asia continental collisional setting and was controlled by a large reverse fault. Field observations reveal that the Mesozoic and Cenozoic sedimentary strata were outcropped in the mining area, and that the orebodies are obviously controlled by faults and hosted in sandstone and carbonate rocks. However, the ore-forming elements in the east ore belt are mainly Pb-Zn -Sr-Ag, while Pb-Zn-Ag-Cu-Co elements are dominant in the west ore belt. Comparative analysis of the C-O-Sr-S-Pb isotopic compositions suggest that both ore belts had a homogeneous carbon source, and the carbon in hydrothermal calcite is derived from the dissolution of carbonate rock strata; the ore-forming fluids were originated from formation water and precipitate water, which belonged to basin brine fluid system; sulfur was from organic thermal chemical sulfate reduction and biological sulfate reduction; the metal mineralization material was from sedimentary strata and basement, but the difference of the material source of the basement and the strata and the superimposed mineralization of the west ore belt resulted in the difference of metallogenic elements between the eastern and western metallogenic belts. The Pb-Zn mineralization age of both ore belts was contemporary and formed in the same metallogenetic event. Both thrust formed at the same time and occurred at the Early Oligocene, which is consistent with the age constrained by field geological relationship.

Key words: eastern Tethyan metallogenic domain, Lanping Basin, Baiyangping ore concentration area, lead-zinc polymetallic ore deposit, genesis of deposit

1 Introduction

The Tethyan metallogenic belt is one of the three global metallogenic domains, which is located between the west of Mediterranean and the Sumatra Islands. It extends up to 10000 km with a very complicated tectonic history and a wide spatial distribution, and hosts multiple types and extraordinary polymetallic concentrations (Zhang Hongrui et al., 2010; Deng et al., 2014a; Deng et al., 2014b; Wang et al., 2014; Hou and Zhang, 2015; Gong Xuejing et al., 2017). Sediment-hosted lead-zinc polymetallic deposits are one of the most important types, including the global largest Media Abad, the second largest Jinding, the fourth largest Reocin Mississippi Valley type (MVT) lead-zinc deposits, and the Upper Silesia MVT lead-zinc ore concentration area (Leach et al., 2005; Xue et al., 2007; Rajabi et al., 2012; Deng et al., 2016).

The Lanping Basin in the Sanjiang area of northeastern margin of the Tibetan Plateau is the major eastern stretch

* Corresponding author. E-mail: wangzykc@yeah.net.

© 2018 Geological Society of China

of the Tethyan metallogenic domain. This basin hosts a number of large unique sediment-hosted Pb-Zn polymetallic deposits, including the Baiyangping ore concentration area which is one of the representative ore district of the Sanjiang belt. The Baiyangping ore concentration area, formed in a folded tectogene of the India-Asia continental collisional setting and controlled by reverse faulting, can be divided into the east and west belts. It is characterized by the presence of clastic and carbonate rocks, and ore-forming elements of Pb, Zn, Cu, Ag, Co, Sb, As, Bi, etc., which are considered atypical for MVT, SEDEX, and SST Pb–Zn deposits, typical polymetallic deposits in a continental collision setting (Xue et al., 2007; Hou Zengqian et al., 2008; He et al., 2009; Feng Caixia et al., 2011; Wang et al., 2015). Efforts have been made to reveal the genesis of deposits in the Baiyangping ore concentration area, including the source of ore-forming fluids and metals as well as the metallogenic epoch (Tian Hongliang, 1997; Chen Kaixu et al., 2000, 2004a, 2004b; Shao Zhaogang et al., 2002, 2003; Zhu Dagang et al., 2002; Xue Chunji et al., 2003; Wang Feng and He Mingyou, 2003; He Mingqin et al., 2004a; Li Zhiming et al., 2004, 2005; Wang Feng, 2004; Wang Yanbin et al., 2004; Xu Qidong and Zhou Lian, 2004; Xu Shihai et al., 2005; He Longqing et al., 2005, 2007; Chen Kaixu, 2006; Yu Fengming et al., 2007, 2011; He Mingyou et al., 2009; Liu Jiajun et al., 2010; XueWei et al., 2010; Feng Caixia et al., 2011; Zou Zhichao et al., 2012; Feng et al., 2014; Zhang et al., 2015; Li Yike et al., 2016).

In general, previous researches were independently conducted on the east or the west ore belt of the Baiyangping area, respectively. The genesis of the overall ore concentration area remains controversial. The origin of complexity and variety of the ore-forming elements and polymetallic combination are not understood; the relationship between the east and west belt is not well addressed.

In this work, the structural characteristics of the host rocks and the ores of the Baiyangping ore concentration area were examined via field surveys. The comparative study of fluid inclusion data, ore-forming fluids, ore-forming materials and metallogenic age of the east and west ore belts was analyzed for discussing the mineralization. In this paper, the differences in the sources of ore-forming fluids and metals in the east and the west belts are addressed to reveal the genesis of polymetallic deposits of the Baiyangping ore concentration area and deepen our knowledge on the origin of sediment-hosted polymetallic deposits in continental collisional setting in the Tethyan metallogenic domain.

2 Tectonic Setting and Regional Geology

2.1 Tectonic setting

The Mesozoic–Cenozoic Lanping Basin is an important part of the Tethyan tectonic domain. The basin is located at a bend of the giant eastern Alps–Himalayan tectonic belt (Fig. 1). There are three suture zones in the ‘‘Sanjiang” region, named the Nujiang, Lancangjiang and Jinshajiang-Ailaoshan suture zones. The Lanping Basin is in the Changdu-Simao microplate, bounded between the Lancangjiang and Jinshajiang-Ailaoshan suture zones. The microplate abuts the Yangtze plate to the west, the Tibet-Yunnan plate to the east, and the Simao Basin to the north, tapering gradually to the north. The Lanping Basin is located in the NNW-striking structural zone of the southern arcuated transition (Fig. 1) (Que Meiying et al., 1998), part of the Hengduanshan syntaxis and associated arcuated transition zone formed in the collision between the Indian and the Eurasian plates as well as the stopping of the Yangtze plate.

2.2 Stratigraphy

The sedimentary cover of the Lanping Basin is composed of Mesozoic and Cenozoic carbonates and clastic rocks. It consist of the Middle Triassic Shanglan (T_2s) and Pantiange (T_2p) formations; the Upper Triassic Waigucun (T_3w), Sanhedong (T_3s), and Maichuqing (T_3m) formations followed by a sedimentary hiatus; the Middle Jurassic Huakaizuo (J_2h) formation; Upper Jurassic Bazhulu (J_3b) formation; the Lower Cretaceous Jingxing (K_1j), Nanxing (K_1n), and Hutousi (K_1h) formations followed an Upper Cretaceous hiatus; the Eocene Yunlong (E_1y), Guolang (E_2g), and Baoxiangsi (E_2b) formations; and a non-subdivided Upper Eocene sedimentary sequence (Qin Gongjiong and Zhu Shangqing, 1991; Mou Chuanlong et al., 1999; Xue Chunji et al., 2002; Feng et al., 2014). The Proterozoic metamorphic basement is exposed along and outside the boundary faults of the basin (Figs. 2 and 3).

2.3 Structures

The structural style of the Lanping Basin is highlighted by two nearly N-S trending thrust faults, shallowly dipping to the east and the west, respectively (Figs. 2 and 4). Structural analysis revealed that these nappe systems were overthrusted over the Tertiary clastic rocks (E_1, E_2) in an antithentical E-W directed shortening in Cenozoic time (He et al., 2009). The Pb-Zn polymetallic deposits in Lanping Basin are distributed along the west and east thrust faults, respectively (Fig. 2).

2.4 Magmatic activity

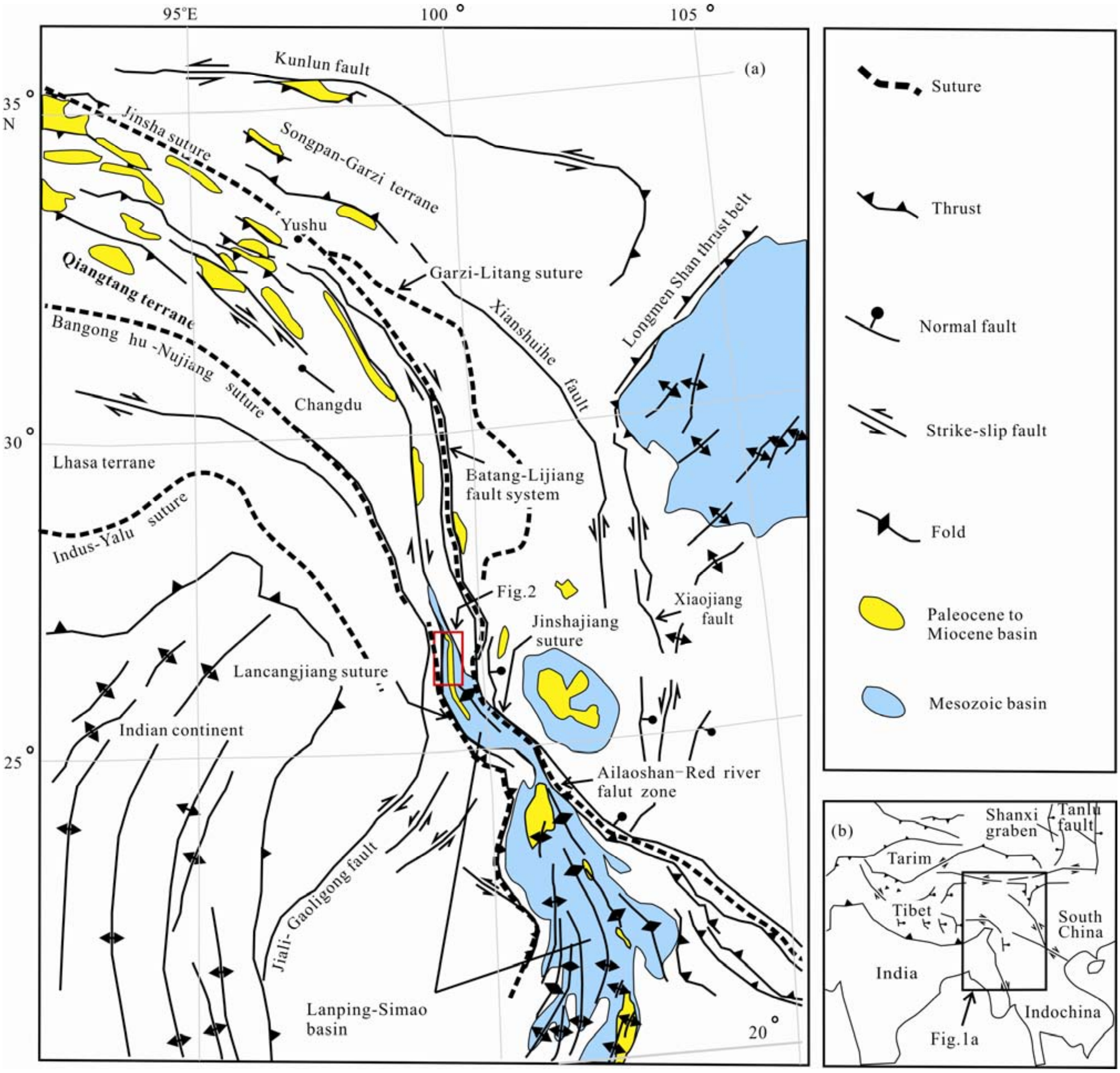

Fig. 1. Cenozoic tectonic map of eastern Tibet and Indochina, showing the structure systems and distribution of Mesozoic to Cenozoic basins (modified from Wang et al., 2001).

Limited magmatic rocks have been discovered in the Lanping Basin. Paleozoic intermediate-acid volcanic rocks are distributed along Langcangjiang fault zone, considered as the Late Carboniferous and Early Permian active island arc assemblages (Tan Fuwen et al., 1999; Li Mei, 2004). The Mesozoic magmatic activity is represented by Triassic intermediate-acidic extrusives with limited amount of intrusives, distributing along the Jinshajiang-Ailaoshan fault zone of eastern margin of the Lanping Basin. In addition, the Yanshanian intermediate-acid intrusives develop along east and west margins of the basin. The biotite monzonite granite, biotite granite, moyite and a small amount plagiogranite were formed mainly in the southern section of the Jinshajiang-Ailaoshan fault zone (Fan Weiming, 1992; QueMeiying et al., 1998; He Mingqin et al., 2004b; Zeng Rong, 2007). The Cenozoic magmatism is marked by the Himalayan alkaline intrusives along the margin of the basin, e.g., the Zhuopan pluton of 36–39 Ma (Dong Fangliu et al., 2005; Zeng Pusheng et al., 2006), the Yongping pluton of 41–27 Ma (Qian Xianggui and Lü Boxi, 2000), and scattered plutons in the basin ranging from 36.7 to 46.5 Ma (Zhang Chengjiang et al., 2000; Teng Yanguo et al., 2001; Zhao Haibin, 2006).

2.5 Tectonic evolution

The Lanping Basin underwent a complicated tectonic history, which can be summarized as a three-stage

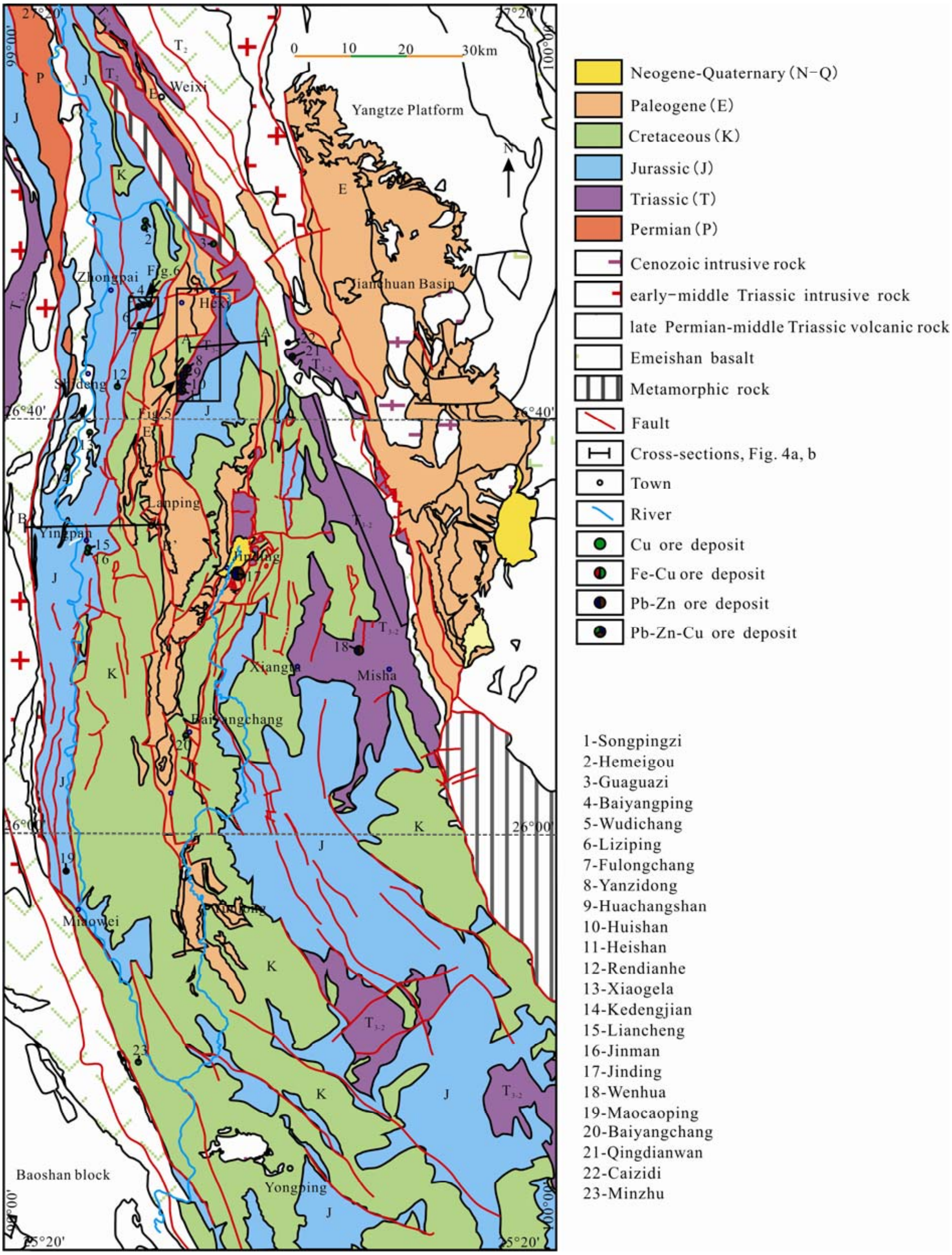

Fig. 2. Geological map of the Lanping Basin and surrounding regions (modified ftom two 1:200,000 geological maps of the Yongping, Lanping and Weixi areas (YBGMR, 1974, 1984).

evolution based on previous studies (Liu Zengqian et al., 1983; Li Xingzhen et al., 1999; Mou Chuanlong et al., 1999; Pan Guitang et al., 2003; He et al., 2009). A Late-Triassic rift basin: It was produced in back-arc extension in Mid- Late Triassic time (Mo Xuanxue et al., 1993; Pan Guitang et al., 2003), induced by the closure of the Paleo-

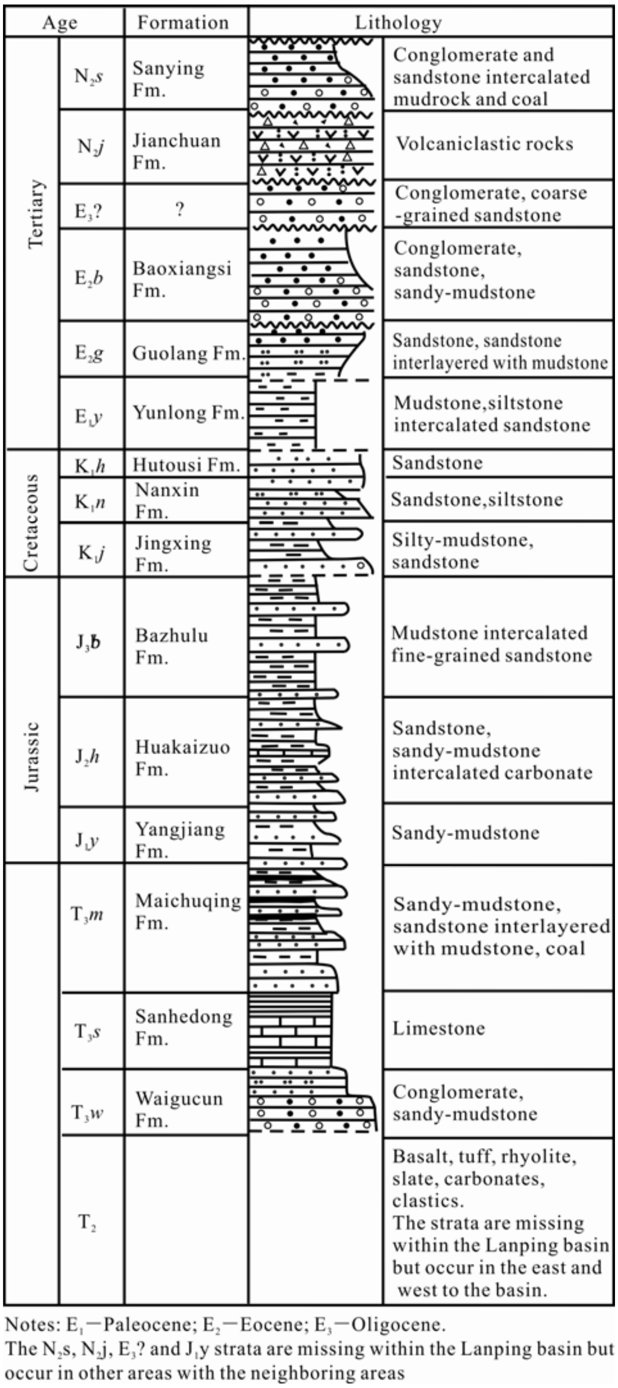

Fig. 3. Stratigraphic column of the Lanping Basin (Mou Chuanlong et al., 1999).

Tethyan ocean in the early Triassic time (Liu Zengqian et al., 1993; Mo Xuanxue et al., 1993; Li Xingzhen et al., 1999). Bimodal volcanic and shallow marine sedimentary rocks highlight the basin sequence (Fig. 3) (Mou Chuanlong et al., 1999). A Jurassic–Cretaceous depression basin: It was generated in E-W shortening associated with the opening of the Bangong-Nujiang ocean in the Jurassic (Liu Zengqian et al., 1993) and the closing of the Garzê-Litang oceanic basin at the end of Triassic (Hou Zengqian et al., 1995). Red beds make the main cover of the basin during that time. A Tertiary foreland basin: It is resulted from the Indo-Asian collision activated at ca. 65–50 Ma. As one of the isolated Tertiary foreland basins along the eastern edge of the Tibetan Plateau (Fig. 1) (Wang et al., 2001; Spurlin et al., 2005; Li Yalin et al., 2006), the transition from a depression to a foreland basin of the Lanping Basin is considered being achieved before 51 Ma in eastern Tibet (Spurlin et al., 2005). Cenozoic molasses, lacustrine, and fluvial deposit filled up the basin (Fig. 3) (Mou Chuanlong et al., 1999).

3 Geology of the Baiyangping Ore Concentration Area

The east ore belt consists of the Hexi, Dongzhiyan, Xiaquwu, Yanzidong, Huachangshan, Huishan, and Heishan ore deposits/blocks, which are located along the NNE-striking Huachangshan thrust fault (Figs. 2 and 5; Table 1). The west ore belt consists of the Baiyangping, Liziping, Wudichang and Fulongchang ore blocks (Fig. 6). The ore bodies are hosted in Mesozoic sandstones and carbonates, and occur in three faults of nearly North-South (N-S-striking), West-Northwest (WNW), and Northeast-Southwest (NE-SW), respectively (Fig. 6; Table 1).

3.1 Ore-host strata

The clastic and carbonate rocks of the Upper Triassic Sanhedong (T_3s), Waluba (T_3wl), and Maichuqing (T_3m) formations as well as clastic rocks of the Cenozoic Yunlong (E_1y), Guolang (E_2g), and Baoxiangsi (E_2b) formations are exposed in the east ore belt. The major ore-hosting units are of the Upper Triassic Sanhedong carbonates (T_3s), the Paleocene Yunlong sandstone (E_1y), and the Eocene Baoxiangsi sandstone (E_2b).

In the west ore belt, the Middle Jurassic Huakaizuo formation (J_2h) is composed of carbonate-bearing silty mudstone, siltstone, and sandstone, which is overlain disconformably by the Lower Cretaceous Jingxing formation (K_1j) of quartzose sandstone, siltstone, and variegated mudstone. Medium-bedded and medium-fine grained lithic sandstone, siltstone, and mudstone of the Lower Cretaceous Nanxing formation (K_1n) is exposed on top of the Jingxing formation. The host rocks of the Liziping, Wudichang, and Fulongchang ore blocks are marls and bioclastic limestones of the Huakaizuo formation with minor amount of bioclastic limestones of the Jingxing formation. The host rock of the Baiyangping ore block is mainly calcareous sandstone of the Jingxing formation.

3.2 Ore-controlling structures and host structures

The distribution of orebodies in the eastern belt are

Table 1 Geology and features of each block in the Baiyangping ore concentration area

Name	Ore block	Metallic Comm.	Tonnage	Grade	Structural control	Host Rocks	Alteration	Ore textures	Mineral assemblage	Orebody Shape	Data Source
East ore belt	Hexi	Sr-Pb-Zn	/	/	Huachangshan fault	Sanhedong Fm. dolomitic limestone	Cel. Cal. Dol.	Massive, breccia	Celestite, galena, sphalerite	stratiform-like lenticular	Chen Kaixu, 2006
	Dongzhiyan	Ag-Cu	/	Ag: 165–189 g/t Cu: 0.38–1.59wt%	Huachangshan fault	Sanhedong Fm. dolomitic limestone	Dol. Cal.	Massive, breccia	Celestite,	stratiform-like lenticular	Chen Kaixu, 2006; Zhao Haibin, 2006
	Xiaquwu	Ag-Cu	/	Ag: 165–189 g/t Cu: 0.38–1.59wt%	Huachangshan fault	Sanhedong Fm. dolomite, Yunlong and BaoxiangsiFms. sandstone, conglomerate.	Cal. Dol.	Massive, breccia	Tetrahedrite, azurite, argentite, pyrite	stratiform-like lenticular	Song Yucai, 2009
	Yanzidong	Zn-Pb-Ag-Cu	/	Ag: 165–189 g/t Cu: 1.3wt% (average) Pb: 1.95wt% (average) Zn: 2.41wt% (average)	Huachangshan fault	Sanhedong Fm. dolomite, Yunlong and BaoxiangsiFms. sandstone, conglomerate.	Cal. Dol. Si.	Massive, breccia	Sphalerite, galena, celestine, copper oxide	stratiform-like lenticular	Chen Kaixu, 2006; Song Yucai, 2009
	Huachangshan	Pb-Zn-Ag	Zn+Pb: >0.5 Mt Ag: >3000 t Cu: ~0.3 Mt	Cu: 1.11–1.81g/t Ag: 15.8 g/t (average) Pb: 1.46wt% (average) Zn: 1.60wt% (average)	Huachangshan fault	Sanhedong Fm. dolomitic limestone	Cal. Dol. Si.	Massive, breccia	Galena, sphalerite, pyrite, calcite	stratiform-like lenticular	Chen Kaixu, 2006; Song Yucai, 2009
	Huishan	Pb-Zn-Ag	/	Ag: 114.9 g/t Pb: 3.55wt% Zn: 2.36%	Huachangshan fault	Sanhedong Fm. dolomitic limestone	Cal. Si.	Massive, breccia	Galena, sphalerite, pyrite, fluorite, calcite	stratiform-like lenticular	Song Yucai, 2009
	Heishan	Pb-Zn-Ag	/	Ag: 23.3 g/t (average) Pb: 1.27wt% (average) Zn: 3.39%(average)	Huachangshan fault	Sanhedong Fm. dolomitic limestone	Cal. Si.	Massive, breccia	Galena, sphalerite, calcite	stratiform-like lenticular	Song Yucai, 2009
West ore belt	Liziping	Pb-Zn-Ag	/	Pb:3.51–5.29wt% Zn:2.66–6.32wt% Ag: 82.85–153.06 g/t	WNW striking faults	Jurassic Marl, and bioclastic limestone	Cal, Si	Massive, thin vein, breccia	Sphalerite, gratonite, galena, jordanite, realgar and orpiment	stratiform-like	Kong Yunli and Qi Linkun, 2009; Deng Shuangling, 2011
	Wudichang	Zn-Pb-Ag	/	Ag: 89–255 g/t Pb: 4.2–10.4wt% Zn: 15.33–12.2wt% Cu: /	NE striking Faults and NW fractures	Jurassic Marl and bioclastic limestone	Cal, Si, Arg	Massive, thin vein, breccia	Sphalerite, gratonite, galena, jordanite, realgar and orpiment	Lenticular,stratiform-like	Chen Kaixu, 2006
	Fulongchang	Cu-Pb-Zn- Ag	Ag:~2000 t Cu:0.12 Mt	Ag: 328–547 g/t Pb: 4.2–7.3wt% Zn: / Cu: 0.63–11.70wt%	Second-order NE Striking faults; the front zone in the western thrust-nappe system	Cretaceous transitional zone between porous sandstone and low-permeability carbargillite	Si, Ca	Net vein, disseminated, breccia	Sphalerite, jordanite, galena, tetrahedrite series minerals, bournonite, argentite and kongsbergite,	Lenticular,stratiform-like	Chen Kaixu, 2006
	Baiyangping	Cu-Co-Ag	/	Ag: / Pb: / Zn:/ Cu: 0.86–3.3wt% Co: 0.10–0.27wt%	Second-order NE striking faults; the front zone in the western thrust-nappe system	Cretaceous transitional zone between porous sandstone and low-permeability carbargillite	Si, Ser, Ca, Epi	Massive, breccia	Tetrahedrite series minerals, chalcocite, chalcopyrite, jordanite, cobaltine, siegenite cobalt-bearing arsenopyrite, galena, sphalerite	stratiform-like lenticular	Chen Kaixu, 2006

Alteration abbreviations: Arg, Argillization; Si, Silicification; Ser, Sericitization; Ca, Carbonatization; Epi, Epidotization; Cal, Calcitization; Dol, Dolomitization; Cel, Celestite. /, No data.

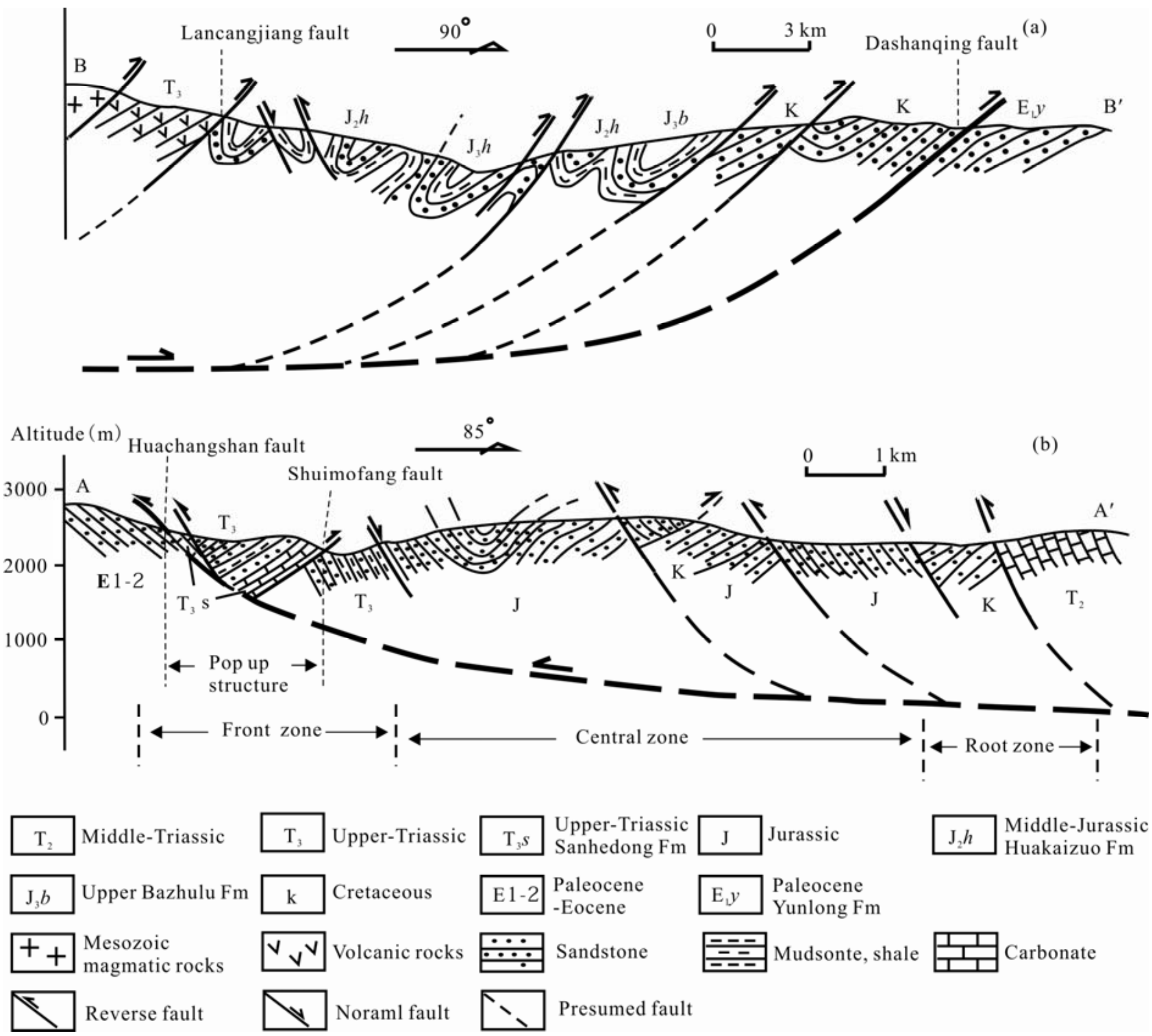

Fig. 4. Geological cross-sections of AA' and BB' in the northern Lanping Basin, showing the frameworks of (a) the western and (b) the eastern thrust-nappe systems, respectively. See AA' and BB' in Fig 2 (after He Longqing et al., 2009).

controlled by the Huachangshan thrust, dipping to 110° with dip angles between 30° and 40° (He Longqing et al., 2004). The hanging wall and foot wall are composed of the Late Triassic Sanhedong limestone and Cenozoic clastic rocks, respectively. Ore bodies are hosted mostly in intendively developed fractures, breccia zone and karst caves of the limestone.

In the west ore belt, at the scale of the ore zone, there are three groups of faults, including the N-S-striking Sishiliqing thrust fault (Fig. 6), the NE-striking faults of F6–F9 and F12, and the WNW strike-slip fault F5 that offsets the two former groups (Fig. 6a). The WNW-trending fault F5, dipping from 210° to 240° at the angles of 20° to 40° as the ore-controlling fault of Liziping ore block, was initially a revers fault that was re-activated as a normal fault (Wang Xiaohu et al., 2011b). The NE-SW trending faults were considered right-lateral compresso-shear first and were transformed to left-lateral tenso-shear later (Tian Hongliang, 1997), acting as the ore-controlling faults of the Wudichang, Fulongchang, and Baiyangping ore blocks (Figs. 6a, b), with a dip angle of about 70°. The open-space filling and replacement are the main mineralization styles.

3.3 Characteristics of the orebodies

Over 20 orebodies in lenticular, nest-like, and beaded shapes are exposed along the Huachangshan fault. Generally, the orebodies are of 135–3500 meters in length and 2.3–16.9 meters in thicknesses with the average grades of 0.8%–3.6% of Pb, 1.6%–3.3% of Zn, 23.3 g/t–220.1 g/t of Ag, and 0.2%–1.9% of Cu (Chen et al., 2004a).

In west ore belt, vein orebodies are observed mainly in three fault zones; their distributions are concordant with the geometry and the orientation of the fault. The thickness of the WNW-striking F5 fault zone, the lead-zinc orebody controlling fault in the Liziping ore block, ranges from centimeters to a few meters with 3.51%–5.29% of Pb, 2.66%–6.32% of Zn, and 82.85–153.06 g/t of Ag (Deng Shuangling, 2011). In the Wudichang ore block, the distribution of the stratiform-like ore veins composed of lenticular orebodies is controlled by NW-trending fractures and NE-striking faults with 4.2%–10.4% of Pb, 12.2%–15.33% Zn, and 89 g/t–255 g/t of Ag. The distributions of the orebodies in the Fulongchang ore block and the Baiyangping block are controlled by the NE-striking fault with 0.63%–11.70% of Cu, 4.2%–7.4% of Pb, and 328 g/t–547 g/t of Ag in Fulongchang and 0.86%–3.3% of Cu, 0.10%–0.27% of Co, and 3.0 g/t–33.8 g/t Ag in Baiyangping, respectively (Chen Kaixu, 2006; Zhao Haibin, 2006).

3.4 Ore characteristics and mineral assemblages

In east ore belt, the ore composition is of celesite associated galena or only celesite in Hexi; celesite associated galena and sphalerite in Yanzidong; galena and sphalerite in Huishan, and copper oxide with relatively higher Ag content in Xiaquwu and Yanzidong. Ore structures are brecciated, stockworked, finely veined, massive, and disseminated; crustuformed, net-like, and grape-like in oxidation zone. Mineral textures are metasomatically relict, euhedral- xenomorphic granual, cataclastic, and recrystallized etc., indicating activities of hydrothermal fluids. Ore minerals are composed of copper-bearing minerals, such as tetrahedrite series, chalcocite, tenorite, chalcopyrite, bornite, malachite, azurite, and covellite; lead-bearing minerals, such as galena, bournonite, cerussite, and anglesite; zinc-bearing minerals, such as sphalerite and smithsonite; and Sr-bearing mineral celesite, with minor pyrite and marcasite. The gangue minerals were calcite, dolomite, barite, fluorite, quartz, and clay minerals (Chen Kaixu et al., 2000; He et al., 2009). Mineralization in the study area is associated with dolomitization, calcification, silicification, and pyritized alteration. The weak wall rock alteration and simple alteration mineral assemblages indicate a middle-low temperature hydrothermal mineralization (Fig. 7).

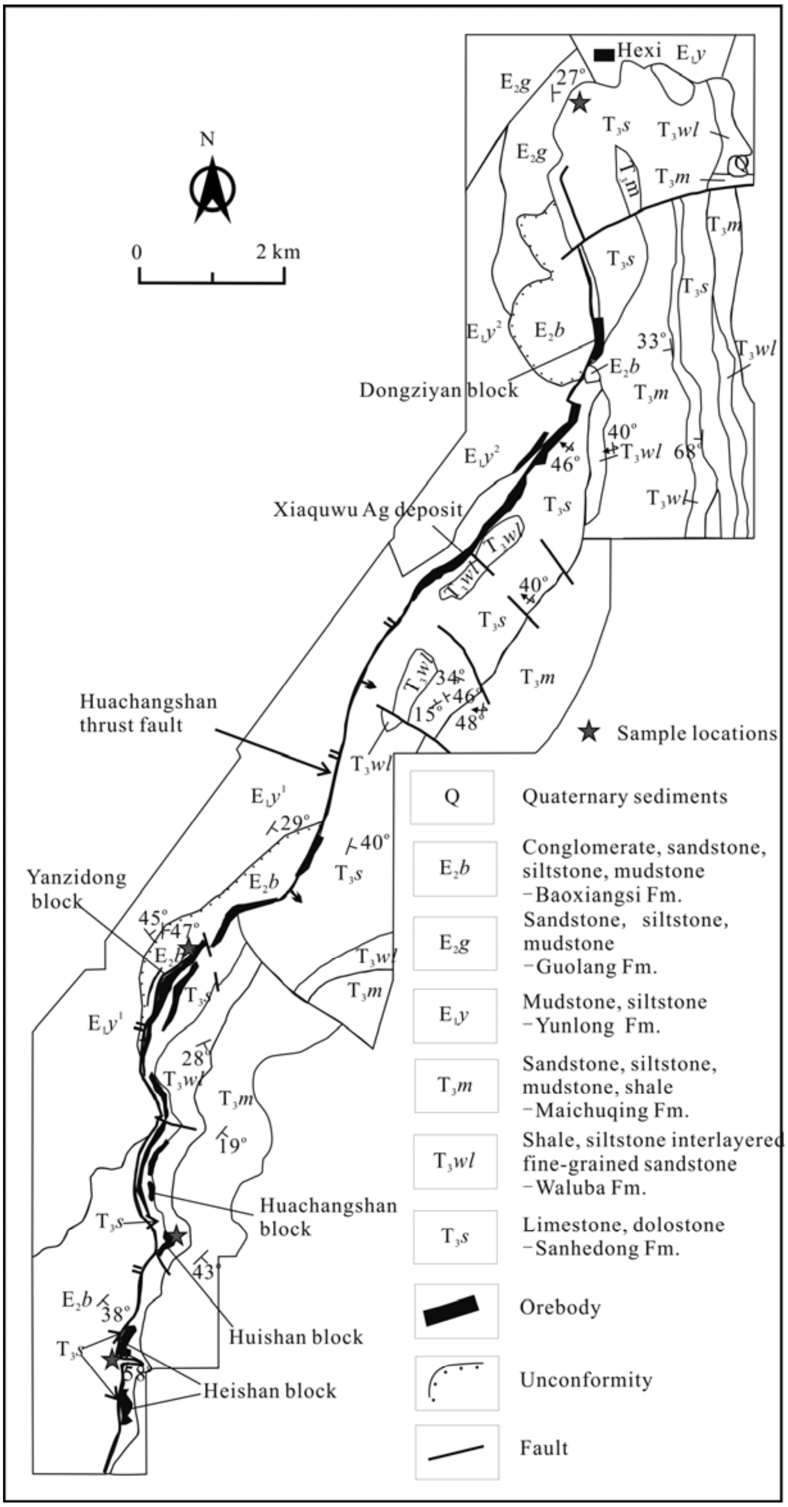

Fig. 5. Geological map of east ore belt of Baiyangping polymetallic ore district (after Chen Kaixu, 2006; Zhao Haibin, 2006).

In west ore belt, ore-forming minerals are mainly composed of sulfides, sulfosalts, sulfates, and oxided minerals. Oxidized ores are smithsonite, malachite, azurite, and limonite in the leached zone or at surface with veinlet-banded, honeycomb, and crustiform structures.

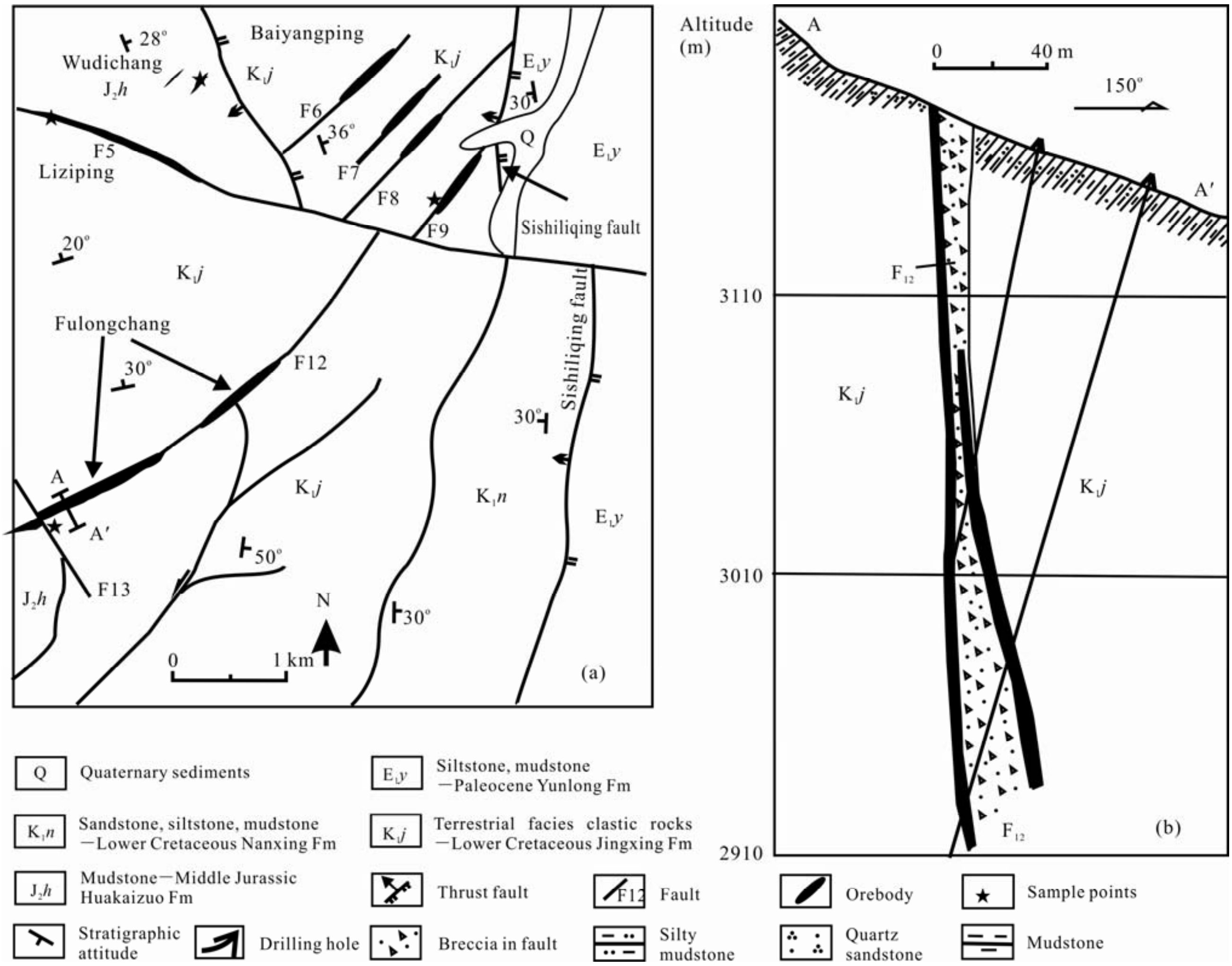

Fig. 6. Geological map with locations of ore bodies of west ore belt in Baiyangping polymetallic ore district (modified from Tian Hongliang, 1997).

The primary ores are characterized by massive, brecciated, disseminated, and vein textures. Massive, breccia, and veined textures indicate an epigenetic hydrothermal mineralization. Compositions of mineral and element vary among different ore blocks. The major ore-forming minerals are sphalerite, gratonite, galena, jordanite, realgar, and orpiment with Pb-Zn-As-Sb-Ag enrichment in Liziping and Wudichang blocks; sphalerite, jordanite, galena, tetrahedrite series, bournonite, argentite, and kongsbergite with enriched Pb-Zn-Cu-Ag in Fulongchang; and, tetrahedrite series, chalcocite, chalcopyrite, jordanite, cobaltine, siegenite cobalt-bearing arsenopyrite, galena, and sphalerite with Cu-Co-As-Ag-Zn-Pb in Baiyangping block (Wang et al., 2015).

4 Samples and Methods

The fresh samples were collected from the east and west ore belts. The detailed sampling localities are shown in Figs. 5 and 6a.

The carbon and oxygen isotope compositions of the siderite samples were analyzed using the MAT-253 mass spectrometer at the CNNC Beijing Reasearch Institute of Uranium Geology. The test was conducted using the phosphoric acid method (DZ/T0184.17–1997) which gave the data accuracy ± 0.2‰.

The Sr isotope compositions of the calcite and celestine samples were analyzed using the MAT-252 mass spectrometer at the State Key Laboratory for Mineral Deposit Research, Nanjing University. Sr isotopic reference material is NIST SRM 987. Average of 0.710260±5 was given on different days.

The sulfur isotope measurements on the sulfide minerals were performed on powders made from ore samples. The samples were analyzed using a Delta V Plus mass spectrometer at CNNC Beijing Research Institute of Uranium Geology. The process of the experiment is as follows: Pure samples of 200 mesh were selected, mixed with cuprous oxides according to a certain proportion, and heated in the vacuum up to 2.0×10^{-2} Pa. The sulfur

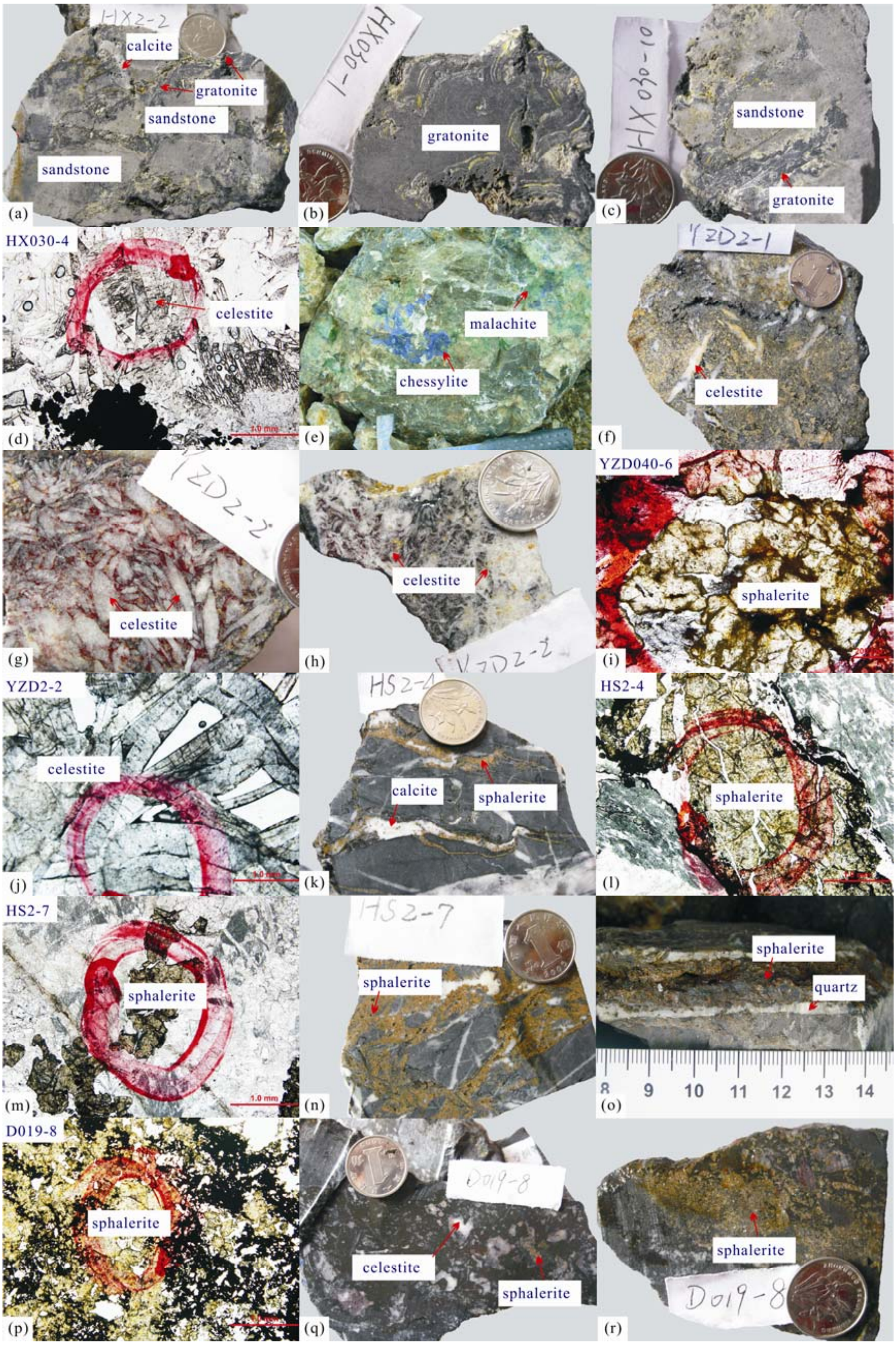

Fig. 7. Ore compositions of the east ore belt in the Baiyangping polymetallic ore district.

dioxide gas is generated when the reaction temperature reaches 980°C, under the vacuum condition, sulfur dioxide gas was collected by the freezing method, and the sulfur isotope composition was analyzed by Delta V Plus gas isotope mass spectrometry. The results were recorded as $\delta^{34}S_{V\text{-}CDT}$ (‰) with V-CDT as the standard. The analysis accuracy is better than ±0.2‰ (2σ).

The Pb isotope test work was done at CNNC Beijing Reasearch Institute of Uranium Geology. The 200 mesh samples were prepared for testing, dissolved by mixed acid ($HF+HClO_4$). The Pb was separated by resin exchange method. The Pb isotope was measured by analytical instrument of ISOPROBE-T after evaporating to dryness. The analytical precision is better than 0.005%.

5 Results

In this test, the $\delta^{13}C_{PDB}$ and $\delta^{18}O_{SMOW}$ values of the siderite from the Baiyangping ore block range from –5.9‰ to –5.7‰ and 17.0‰ to 20.3‰ with averages of –5.8‰ and 18.2‰, respectively (Table 2).

The Sr isotope data of ore-forming stage calcite and celestine are shown in Table 2. In the east belt, the Sr isotopic values of calcite and celestine are in the ranges of 0.708280 to 0.709633 and 0.707669 to 0.710115 with the averages of 0.709285 and 0.709341, respectively. In the west ore belt, the Sr isotopic value of calcite ranges from 0.708323 to 0.711267 with an average of 0.709895.

In this test, the $\delta^{34}S$ values of sulfide range from 3.7‰ to 7‰ with an average of about 5.5‰ at the Baiyangping ore block. The $^{206}Pb/^{204}Pb$, $^{207}Pb/^{204}Pb$, and $^{208}Pb/^{204}Pb$ values range from 18.604 to 18.736, 15.635 to 15.804, and 38.854 to 39.414, respectively (Table 3).

6 Discussions

6.1 The mineralization age and thrust activities

The Lanping Basin, characterized by complex folds and fractures, was considered formed in Tertiary time syntectonically with the eastern and western thrust systems (Tao Xiaofeng et al., 2002; Fu Xiugen, 2005; He et al., 2009). The lead-zinc polymetallic deposits in the northern Lanping basin distribute mainly along these two thrust systems, such as the Fulongchang, Baiyangping,

Table 2 C-O-Sr isotope composition of carbonate minerals from the Baiyangping ore concentration area

Name	Ore block	Sample No.	Mineral/Rock	$\delta^{13}C_{PDB}$(‰)	$\delta^{18}O_{PDB}$(‰)	$\delta^{18}O_{SMOW}$(‰)	$^{87}Sr/^{86}Sr$	SE
West ore belt	Liziping	LZP021-1	Calcite				0.708896	5
		LZP021-5	Calcite				0.708323	6
		LZP2-1	Calcite				0.708779	8
		LZP2-6-1	Calcite				0.708822	4
	Wudingchang	LP08-43	Calcite				0.710990	5
		LP08-45	Calcite				0.710729	5
		WDC022-4	Calcite				0.710252	5
		2WDC2-15	Calcite				0.709647	5
	Fulongchang	FLC2-2	Calcite				0.711240	4
		FLC2-3-3	Calcite				0.711267	5
	Baiyangping	LP14004-1	Siderite	−5.7	−13.2	17.3		
		LP14004-2	Siderite	−5.9	−13.0	17.5		
		LP14004-3	Siderite	−5.9	−12.1	18.4		
		LP14004-10	Siderite	−5.7	−10.3	20.3		
		LP14004-11	Siderite	−5.8	−11.0	19.5		
		LP14004-15	Siderite	−5.9	−12.9	17.6		
		LP14004-16	Siderite	−5.7	−13.4	17.0		
East ore belt	Hexi	HX024-1	Celestine				0.710115	3
		HX024-2	Celestine				0.709926	5
		HX024-3	Celestine				0.709896	6
		HX024-4	Celestine				0.707669	7
		HX024-5	Celestine				0.709971	5
		HX030-4	Celestine				0.709981	4
		HX2-11	Celestine				0.709899	3
		HX2-12	Celestine				0.709977	5
		HX2-14	Celestine				0.709746	4
	Yanzidong	YZD040-5	Celestine				0.708749	5
		YZD040-6	Celestine				0.708660	4
		YZD040-10	Celestine				0.708675	5
		YZD2-1	Celestine				0.708173	6
	Huishan	HS016-7	Calcite				0.709508	6
		HS016-8	Calcite				0.708280	5
		HS016-10	Calcite				0.709477	4
		HS016-12	Calcite				0.709482	5
		HS2-7	Calcite				0.709475	5
		HS2-10	Calcite				0.709633	5
	Heishan	D019-4	Calcite				0.709331	4
		D019-9	Calcite				0.709093	4

Table 3 S-Pb isotope composition of sulfide and sulphosalts from the Baiyangping Pb-Zn polymetallic ore concentration area

Sample No.	Sample description	Mineral	$\delta^{34}S_{V-CDT}$(‰)	$^{206}Pb/^{204}Pb$	$^{207}Pb/^{204}Pb$	$^{208}Pb/^{204}Pb$	Data sources
Fulongchang							
FLC054-5	Galena, sphalerite and quartz vein	Sphalerite	5.9	18.67	15.667	38.975	Wang et al., 2015
FLC054-8	Vein sphalerite	Sphalerite	5.4	18.65	15.618	38.889	Wang et al., 2015
FLC2-8	Massive sphaleriteore	Sphalerite	6.5	18.725	15.72	39.135	Wang et al., 2015
FLC2-21	Coarse-grained sphalerite and fine-grained galena cemented sandstone breccia	Sphalerite	5.8	18.609	15.597	38.74	Wang et al., 2015
FLC2-23	Vein coarse-grained sphalerite	Sphalerite	7.8	18.645	15.64	38.906	Wang et al., 2015
FLC149		Sphalerite	10.5	18.643	15.618	38.811	He Mingqin et al., 2004b
FLC160		Sphalerite	10	18.634	15.604	38.768	He Mingqin et al., 2004b
FLC176		Sphalerite	11.2	18.622	15.548	38.514	He Mingqin et al., 2004b
		Sphalerite	2.45	18.690	15.685	39.018	YBGMR, 1995
FLC054-3	Galena cemented sandstone breccia	Galena	5	18.644	15.638	38.874	Wang et al., 2015
FLC054-7	Galena and quartz vein in sandstone	Galena	4.6	18.648	15.637	38.906	Wang et al., 2015
FLC2-3-1	Galena veinlets	Galena	5	18.687	15.679	39.092	Wang et al., 2015
FLC2-10	Sulphide cemented sandstone breccia	Galena	5.8	18.651	15.65	38.919	Wang et al., 2015
FLC2-20	Galena cemented sandstone breccia	Galena	4.4	18.656	15.662	38.973	Wang et al., 2015
H80		Galena	5.03	18.686	15.677	39.008	Chen Kaixu, 2006
		Galena	−5.64	18.673	15.655	38.943	YBGMR, 1995
		Galena		18.672	15.652	38.927	Pan Guitang, et al., 2003
		Galena		18.680	15.663	38.963	Pan Guitang, et al., 2003
FLC2-2-2	Pyrite and gratonite vein	Pyrite	−10.2	18.654	15.667	38.968	Wang et al., 2015
FLC147		Tetrahedrite	9.2	18.654	15.634	38.862	He Mingqin et al., 2004b
FLC161		Tetrahedrite	7.9	18.644	15.610	38.786	He Mingqin et al., 2004b
H-1		Tetrahedrite	3.5				Li Zhiming et al., 2005
H-3		Tetrahedrite	4.7				Li Zhiming et al., 2005
Liziping							
LZP021-2	Massive sphalerite, galena and gratonite ore	Sphalerite	5	18.722	15.666	39.051	Wang et al., 2015
LZP2-2	Calcite-bearing spalerite vein	Sphalerite	5.6	18.745	15.674	39.062	Wang et al., 2015
LZP2-6-1	Sphalerite and calcite vein	Sphalerite	3.8	18.62	15.597	38.716	Wang et al., 2015
LZP2-9-1	Galena and sphalerite ore	Sphalerite	4.6	18.697	15.675	39.007	Wang et al., 2015
LZP1-1		Sphalerite		18.692	15.685	39.037	Zhao Haibin, 2006
LZP021-1	Gratonite, sphalerite and galena vein	Gratonite	7.2	18.751	15.773	39.312	Wang et al., 2015
LZP021-2	Massive sphalerite, galena and gratonite ore	Gratonite	6.3	18.818	15.842	39.556	Wang et al., 2015
LZP021-3	Massive gratonite ore	Gratonite	6.8	18.708	15.716	39.159	Wang et al., 2015
LZP021-4	Galena, gratonite and calcite vein	Gratonite	6.3	18.671	15.67	38.975	Wang et al., 2015
LZP1-1		Galena		18.682	15.683	39.027	Zhao Haibin, 2006
Wudichang							
LP08-41	Massive sphalerite ore	Sphalerite	5.9	18.720	15.698	39.169	Wang et al., 2015
LP08-42	Massive sphalerite ore	Sphalerite	5.9	18.710	15.695	39.054	Wang et al., 2015
LP08-43	Sphalerite and calcite vein	Sphalerite	5.3	18.707	15.696	39.079	Wang et al., 2015
LP08-44	Sphalerite vein	Sphalerite	6.3	18.629	15.633	38.911	Wang et al., 2015
LP08-45	Sphalerite and calcite vein	Sphalerite	5.7	18.629	15.614	38.871	Wang et al., 2015
WDC022-2	Sphalerite, galena and gratonite ore	Sphalerite	5.8	18.633	15.618	38.822	Wang et al., 2015
WDC022-4	Crystalline sphalerite	Sphalerite	4	18.626	15.609	38.791	Wang et al., 2015
WDC022-5	Sphalerite, galena and gratonite ore	Sphalerite	5.6	18.641	15.609	38.794	Wang et al., 2015
WDC022-8	Sphalerite vein	Sphalerite	4.7	18.704	15.677	39.087	Wang et al., 2015
WDC2-3	Calcite-bearing sphalerite and galena vein	Sphalerite	5.1	18.668	15.647	38.849	Wang et al., 2015
WDC2-7	Sphalerite and galena ore	Sphalerite	5.5	18.665	15.628	38.897	Wang et al., 2015
2WDC2-4	Sphalerite, gratonite and calcite vein	Sphalerite	5.4	18.783	15.741	39.14	Wang et al., 2015
2WDC2-7	Sphalerite vein	Sphalerite	3.9	18.669	15.644	38.947	Wang et al., 2015
2WDC2-9	Sphalerite and gratonite vein	Sphalerite	5.1	18.673	15.668	38.986	Wang et al., 2015
2WDC2-11	Sphalerite and galena ore	Sphalerite	6.3	18.689	15.691	39.08	Wang et al., 2015
2WDC2-15	Sphalerite, gratonite and calcite cemented marl breccia	Sphalerite	5.3	18.728	15.746	39.223	Wang et al., 2015
LZP145		Sphalerite	9	18.685	15.659	38.960	He Mingqin et al., 2004b
WDC022-2	Sphalerite, galena and gratonite ore	Gratonite	4	18.7	15.684	39.151	Wang et al., 2015
2WDC2-4	Sphalerite, gratonite and calcite vein	Gratonite	5.1	18.746	15.756	39.269	Wang et al., 2015
Baiyangping							
LP14005-1		Sphalerite	7.0	39.143	15.722	18.672	This study
LP14005-1		Galena	3.9	39.038	15.695	18.644	This study
LP14005-7		Sphalerite	6.7	39.254	15.758	18.699	This study
LP14005-7		Galena	4.5	38.993	15.676	18.637	This study
LP14005-8		Sphalerite	6.7	39.015	15.688	18.644	This study
LP14005-8		Galena	3.8	38.932	15.66	18.628	This study
LP14005-9		Tetrahedrite	5.9	38.854	15.635	18.604	This study
LP14005-10		Sphalerite	6.8	39.052	15.696	18.65	This study
LP14005-10		Galena	3.7	39.414	15.804	18.736	This study
LP14005-15		Tetrahedrite	5.5	38.989	15.677	18.634	This study

Table 3 Continued 1

Sample No.	Sample description	Mineral	$\delta^{34}S_{V-CDT}$(‰)	$^{206}Pb/^{204}Pb$	$^{207}Pb/^{204}Pb$	$^{208}Pb/^{204}Pb$	Data sources
LP14005-22		Sphalerite	7.0	39.236	15.754	18.701	This study
LP14005-22		Galena	4.9	39.096	15.711	18.663	This study
LP14006-5		Chalcopyrite	1.1	38.815	15.635	18.587	This study
LP14006-6		Chalcopyrite	−1.4	38.947	15.664	18.637	This study
LP14006-7		Chalcopyrite	−1.5	38.912	15.653	18.622	This study
LP14006-9		Chalcopyrite	−2.5	38.99	15.672	18.661	This study
W08		Sphalerite	5.8				Zeng Rong, 2007
W18		Sphalerite	5.8				Zeng Rong, 2007
W52		Sphalerite	6.3				Zeng Rong, 2007
W55		Sphalerite	5.3				Zeng Rong, 2007
F02		Sphalerite	7.1				Zeng Rong, 2007
B4-2		Tetrahedrite	6.71	18.669	15.661	38.948	Wang Feng, 2004
B4-3		Tetrahedrite	6.79	18.626	15.610	38.787	Wang Feng, 2004
B4-4		Tetrahedrite	6.91	18.680	15.709	39.068	Wang Feng, 2004
W23		Tetrahedrite	5.3				Zeng Rong, 2007
F08		Tetrahedrite	6.7				Zeng Rong, 2007
BYP116		Tetrahedrite	9.1	18.644	15.610	38.781	He Mingqin et al., 2004b
BY-3-1		Tetrahedrite	5.8				He Mingqin et al., 2004b
BY-3-2		Tetrahedrite	9.3				He Mingqin et al., 2004b
H125		Tetrahedrite	6.1	18.612	15.605	38.789	Chen Kaixu, 2006
-		Tetrahedrite		18.747	15.754	39.245	Pan Guitang et al., 2003
W39		Stibnite	2.1				Zeng Rong, 2007
W52		Stibnite	5.8				Zeng Rong, 2007
B08		Chalcopyrite	7.4				Zeng Rong, 2007
Hexi							
HX024-2	Galena and celestite ore		−11.2	18.605	15.623	38.812	Wang Xiaohu et al., 2016
HX030-1	Massivegalena	Galena	−20.2	18.598	15.601	38.76	Wang Xiaohu et al., 2016
HX030-1	Massivegalena	Galena	−11.0	18.609	15.619	38.809	Wang Xiaohu et al., 2016
HX030-10	Galena cemented limestone breccia	Galena	−19.1	18.584	15.59	38.706	Wang Xiaohu et al., 2016
HX2-14	Symbiosis of celestite and massive galena	Galena	−10.6	18.588	15.594	38.707	Wang Xiaohu et al., 2016
HX024-1		Celestite	17.2				Wang Xiaohu et al., 2016
HX024-2		Celestite	17.8				Wang Xiaohu et al., 2016
HX024-3		Celestite	17.2				Wang Xiaohu et al., 2016
HX024-4		Celestite	18.3				Wang Xiaohu et al., 2016
HX024-5		Celestite	17.1				Wang Xiaohu et al., 2016
HX030-4		Celestite	17.9				Wang Xiaohu et al., 2016
HX02-11		Celestite	17.1				Wang Xiaohu et al., 2016
HX2-12		Celestite	17.3				Wang Xiaohu et al., 2016
HX2-14		Celestite	18.1				Wang Xiaohu et al., 2016
HXQ103		Celestite	16.6				He Mingqin et al., 2004b
Dongzhiyan							
HX-1		Pyrite	10.1	18.460	15.554	38.619	He Mingqin et al., 2004b
HX-2		Pyrite	10.1	18.247	15.571	38.419	He Mingqin et al., 2004b
HX-4-1		Celestite	18.1	18.421	15.567	38.462	He Mingqin et al., 2004b
H10		Celestite	16.29				Chen Kaixu, 2006
Yanzidong							
YZD2-1	Sphalerite ore	Sphalerite	−9.5	18.6	15.572	38.727	Wang Xiaohu et al., 2016
YZD2-2	Sphalerite ore	Sphalerite	−9.2	18.688	15.642	38.918	Wang Xiaohu et al., 2016
YZD040-2	Sphalerite in marl	Sphalerite	−10.5	18.614	15.591	38.753	Wang Xiaohu et al., 2016
YZD040-3	Sphalerite in limestone	Sphalerite	−10.6	18.661	15.597	38.752	Wang Xiaohu et al., 2016
YZD040-6	The ore of celestite and sphalerite	Sphalerite	−10.8	18.553	15.501	38.54	Wang Xiaohu et al., 2016
YZD040-10	celestite and sphalerite vein	Sphalerite	−13.0	18.681	15.642	38.937	Wang Xiaohu et al., 2016
YZD040-5		Celestite	18.7				Wang Xiaohu et al., 2016
YZD040-6		Celestite	18.6				Wang Xiaohu et al., 2016
YZD040-10		Celestite	18.7				Wang Xiaohu et al., 2016
YZD2-1		Celestite	19.4				Wang Xiaohu et al., 2016
DK-1		Tetrahedrite	−3.2				He Mingqin et al., 2004b
DK-2-1		Pyrite	−0.1				He Mingqin et al., 2004b
DK-2-2		Sphalerite	2.1	18.764	15.894	38.474	He Mingqin et al., 2004b
HX-50		Tetrahedrite	−2.9	18.682	15.668	39.179	He Mingqin et al., 2004b
		Galena		18.610	15.650	38.882	Pan Guitang et al., 2003
		Tetrahedrite		18.569	15.612	38.710	Pan Guitang et al., 2003
		Tetrahedrite		18.613	15.651	38.880	Pan Guitang et al., 2003
Huachangshan							
HCS1-1		Galena		18.777	15.684	38.988	Zhao Haibin, 2006
HCS1-2		Chalcocite		18.743	15.683	38.992	Zhao Haibin, 2006
HCS1-3		Chalcocite	−2.1				
Huishan							
HS2-4	Sphalerite- calcite vein	Sphalerite	−6.7	18.742	15.696	39.018	Wang Xiaohu et al., 2016
HS2-5	Sphalerite- calcite veinlets	Sphalerite	−7.7	18.684	15.633	38.822	Wang Xiaohu et al., 2016
HS2-7	Sphalerite- quartz vein	Sphalerite	−6.2	18.703	15.642	38.822	Wang Xiaohu et al., 2016

Table 3 Continued 2

Sample No.	Sample description	Mineral	$\delta^{34}S_{V-CDT}$(‰)	$^{206}Pb/^{204}Pb$	$^{207}Pb/^{204}Pb$	$^{208}Pb/^{204}Pb$	Data sources
HS2-8	Sphalerite- calcite vein	Sphalerite	−6.4	18.685	15.631	38.844	Wang Xiaohu et al., 2016
HS2-9	Sphalerite - calcite vein	Sphalerite	−6.4	18.725	15.647	38.813	Wang Xiaohu et al., 2016
HS2-10	Disseminated sphalerite in calcite network	Sphalerite	−7.1	18.656	15.616	38.806	Wang Xiaohu et al., 2016
HS2-2		Fluorite		18.489	15.658	38.743	Zhao Haibin, 2006
HS2-2		Calcite		18.600	15.666	38.877	Zhao Haibin, 2006
HS1-1		Whole rock		18.676	15.676	38.925	Zhao Haibin, 2006
H140		Sphalerite	−4.14	18.702	15.710	39.063	Chen Kaixu, 2006
HS116		Sphalerite	0.1	18.777	15.708	39.056	He Mingqin et al., 2004b
HX-48-1		Sphalerite	2.0	18.582	15.659	38.999	He Mingqin et al., 2004b
HX-48-2		Tetrahedrite	1.8	18.705	15.727	39.255	He Mingqin et al., 2004b
HX-24		Celestite		18.569	15.604	38.725	He Mingqin et al., 2004b
HX-48-1		Celestite	17.6				He Mingqin et al., 2004b
		Galena	−3.67				YBGMR, 1995
		Galena	−3.89				YBGMR, 1995
Heishan							
D019-4	Brecciated ore	Tetrahedrite	1.3	18.825	15.788	39.331	Wang Xiaohu et al., 2016
D019-8	Lead-zinc ore	Tetrahedrite	−2.7	18.857	15.82	39.129	Wang Xiaohu et al., 2016
D019-8	Lead-zinc ore	Sphalerite	−2.9	18.716	15.621	38.8	Wang Xiaohu et al., 2016
D019-9	Lead-zinc ore	Tetrahedrite	−4.1	18.856	15.826	39.456	Wang Xiaohu et al., 2016
H135		Tetrahedrite	−5.55	18.682	15.626	38.769	Chen Kaixu, 2006
		Galena	−7.33				YBGMR, 1995
		Galena	−3.97				YBGMR, 1995

Liziping, and Wudingchang ore blocks along the western thrust and its second-order faults (Hou Zengqian et al., 2008; He et al., 2009) and the Hexi, Dongzhiyan, Xiaquwu, Yanzidong, Huachangshan, Huishan, and Heishan ore blocks along the Huachangshan thrust (Tian Hongliang, 1997; Shao Zhaogang et al., 2003; Chen Kaixu, 2006; He Longqing et al., 2005,2007; Hou Zengqian et al., 2008; He et al., 2009) during their activation in Tertiary time. .

In western thrust-nappe system, the youngest mineralized stratum involved in the fold belt is the E_2g, overlain unconformablely by the upper Oligocene Baoxiangsi formation (Mou Chuanlong et al., 1999). This unconformity postdates the activation of the western thrust. Considering the mineralization in the thrust-related secondary fault in Wudichang ore block, the activation of the western thrust should be somewhere between Eocene and Oligocene. Similarly, the youngest mineralized stratum involved in the fold-thrust system is the Eocene Baoxiangsi formation, overlain unconformablely by the upper Oligocene sequence in the east thrust system (YBGMR, 1974; Mou Chuanlong et al., 1999). Metallization occurs in Eocene Baoxiangsi sandstone (E_2b) in Yanzidong ore section (Chen Kaixu, 2006; Zhao Haibin, 2006; He et al., 2009). Given that fact that no mineralization has been discovered in the Oligocene and younger strata in the region (YBGMR, 1974), formation of the ore deposits likely occurred between Late Eocene and Early Oligocene. According to the age data, the lead-zinc metallogenetic ages of both ore belts are on 30–29Ma (Wang Xiaohu et al., 2011a; Wang Xiaohu et al., 2016), which is consistent with our field-based analyses.

6.2 The ore-forming fluids sources of eastern and western ore belts

Comparative study the fluid inclusion data, the fluid inclusions from the two ore belts share many similarities: Small sizes, mainly gas-liquid two-phases, and same homogenization temperatures. However, the salinity and fluid density values from the west ore belt are much higher than those from the east ore belt (Chen Kaixu, 2006; Wang et al., 2015). In the west ore belt, the $\delta^{18}O_{SMOW}$ values of calcite in this study have a sufficient range to intersect with several other potential reservoirs (Figs. 8 and 9). However the $\delta^{18}O_{SMOW}$ values of the ore-forming fluids is in the range of meteoric water, indicating that meteoric water was the one of major components in the ore-forming fluids. Given the likely limited infiltration depth of meteoric water and the presence of more than 10 kilometers of sedimentary thickness, it is likely that some depositional formation water was also involved in the mineralization from the burial compaction of the sedimentation. The $\delta^{18}O_{SMOW}$ values of the ore-forming fluids range between –12.94‰ and 8.05‰ with an average of –3.93‰ (Wang et al., 2015). In east ore belt, the $\delta^{18}O_{SMOW}$ values of calcite and siderite range between 2.9‰ and 24.4‰ with an average of 16.4‰. The $\delta^{18}O_{SMOW}$ values of the ore-forming fluids range between –9.5‰ and 12.0‰ with an average of 4.0‰. The minimum $\delta^{18}O_{SMOW}$ value is –9.5‰, which is in the range of precipitate water; the maximum $\delta^{18}O_{SMOW}$ value of calcite is 24.4‰, in range of sedimentary rock value (Figs. 8 and 9). Combined with the features of ore-forming fluids, it can conclude that the ore-forming fluids are from depositional formation water and atmospheric precipitation (Wang Xiaohu et al., 2016). In the $\delta^{18}O$–$\delta^{13}C$

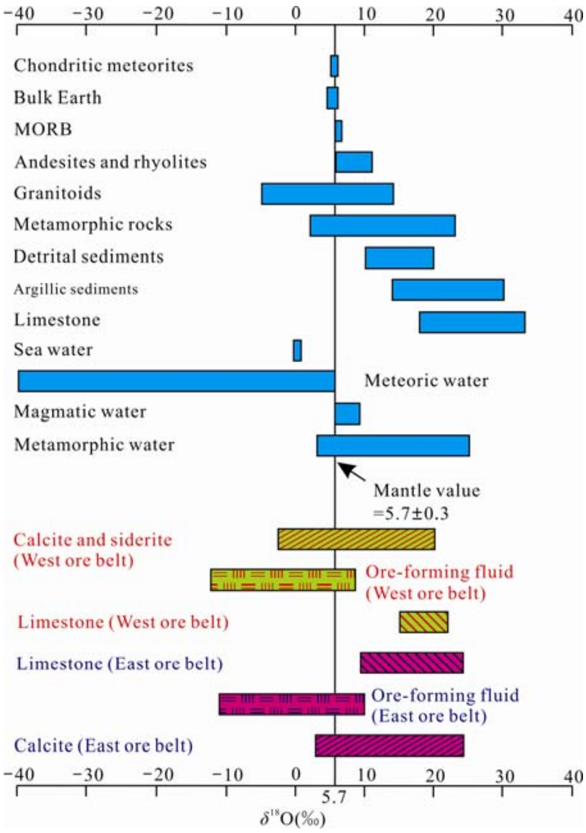

Fig. 8. The δ^{18}O values of carbonate from the Baiyangping Pb-Zn polymetallic ore concentration area and important natural oxygen isotope reservoirs.
Base map from (Rollinson, 1993). Data from (Ye Qingtong et al., 1992; Liu Jiajun et al., 2004; Chen Kaixu, 2006; Wang et al., 2015; Wang Xiaohu et al., 2016).

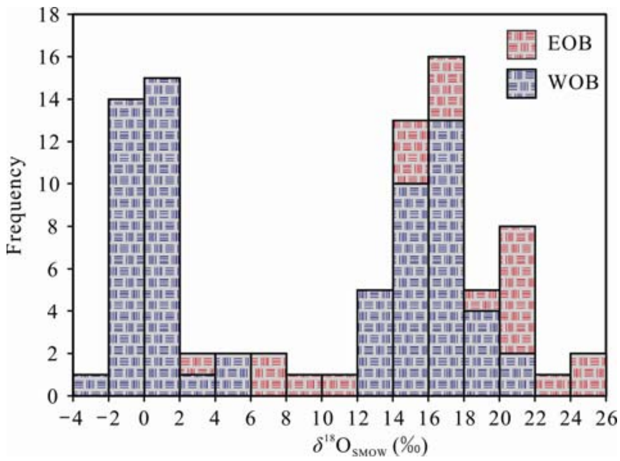

Fig. 9. The comparative map of δ^{18}O values of carbonate from the both ore belts.
Data from (Ye Qingtong et al., 1992; Chen Kaixu et al., 2000; Xue Chunji, 2000; Xue Chunjiet al., 2002; Yang Weiguang, 2002; Yang Weiguang et al., 2003; He Mingqin et al., 2004b; Chen Kaixu, 2006; Zhao Haibin, 2006; Liu Jiajun et al., 2004; Zeng Rong, 2007; Wang et al., 2015; Wang Xiaohu et al., 2016). EOB, East ore belt; WOB, West ore belt.

diagram (Fig. 10), the δ^{18}O values of calcite and siderite from west ore belt are both about magmatic rocks and sedimentary rocks. The δ^{18}O values of calcite from east

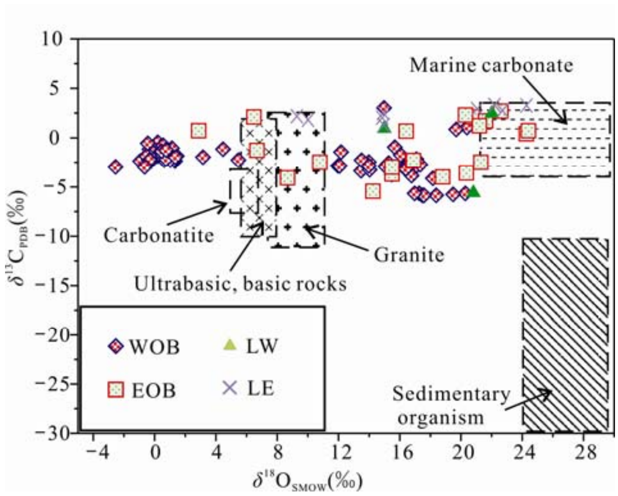

Fig. 10. The C-O values of carbonate from the both ore belts.
Base map from Liu et al. (2004). Data from (Ye Qingtong et al., 1992; Chen Kaixu et al., 2000; Xue Chunji, 2000; Xue Chunji et al., 2002; Yang Weiguang, 2002; Yang Weiguang et al., 2003; He Mingqin et al., 2004b; Chen Kaixu, 2006; Zhao Haibin, 2006; Liu Jiajun et al., 2004; Zeng Rong, 2007; Wang et al., 2015; Wang Xiaohu et al., 2016). EOB, East ore belt; WOB, West ore belt; LW, Limestone of the west ore belt; LE, Limestone of the east ore belt.

ore belt are closer to the value range of marine carbonate, several points fall near the value range of magmatic rocks. In summary, the ore-forming fluids of both ore belts are related to the atmospheric precipitation and depositional formation water, but that flow through different lithologic formations later.

6.3 The ore-forming minerals of eastern and western ore belts

It was proposed that if graphite is not in intergrowth with calcite in hydrothermal veins, the carbon isotopic composition ($\delta^{13}C_{PDB}$) of calcite (or the CO_2 of fluid inclusions) can be approximated as the total carbon isotope composition of hydrothermal fluids (Ohmoto, 1972). The value of the carbon isotopic composition in hydrothermal calcite could be approximated as the total carbon isotopic composition of the hydrothermal ore-forming fluid. In the east ore belt, the $\delta^{13}C_{PDB}$ values of calcite, host rocks, and other carbonate are in the range of –4.1‰ to 2.7‰, 1.26‰ to 3.3‰ and –5.45‰ to 0.67‰, respectively (Xue Chunji, 2000; Yang Weiguang, 2002; He Mingqin et al., 2004b; Liu Jiajun et al., 2004; Chen Kaixu, 2006; Zhao Haibin, 2006; Wang Xiaohu et al., 2016). The $\delta^{13}C_{PDB}$ value of carbonate suggests a marine limestone origin in comparision with the $\delta^{13}C_{PDB}$ value of existing systems (Clark and Fritz, 1997) in the east ore belt. In Figs. 10 and 11, the values of several samples are closed to that of Late Triassic limestone, which indicate that the carbon was from dissolution of carbonate rocks. The $\delta^{13}C_{PDB}$ values of calcite and siderite in the west ore belt range from –4.16‰ to 3‰ and –5.9‰ to –2.95‰,

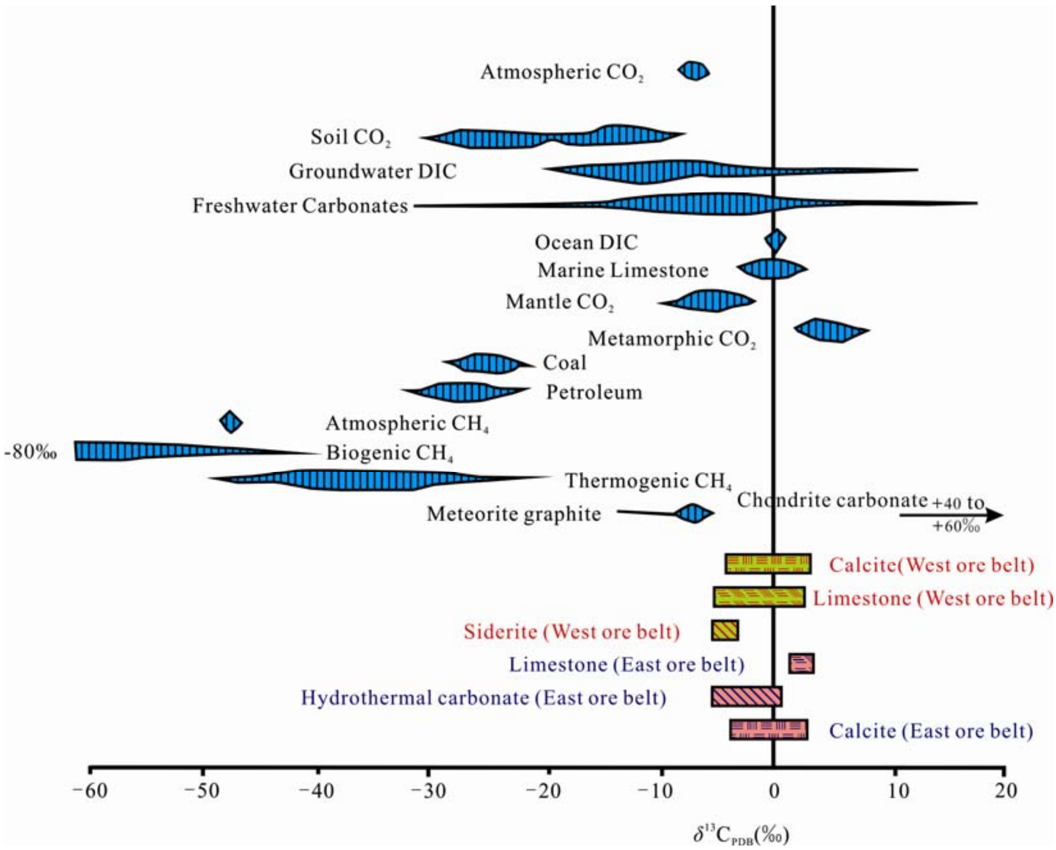

Fig. 11. δ^{13}C values of calcite from the Baiyangping Pb-Zn polymetallic ore concentration area and important geological reservoirs.
Base map from (Clark and Fritz, 1997). Data from (Ye Qingtong et al., 1992; Chen Kaixu et al., 2000; Xue Chunji, 2000; Xue Chunji et al., 2002; Yang Weiguang, 2002; Yang Weiguang et al., 2003; He Mingqin et al., 2004b; Chen Kaixu, 2006; Zhao Haibin, 2006; Liu Jiajunet al., 2004; Zeng Rong, 2007; Wang et al., 2015; Wang Xiaohu et al., 2016).

respectively, which are also close to the $\delta^{13}C_{PDB}$ values of Late Triassic limestones (–5.46‰ to 2.63‰) and carbonatite (Figs. 10 and 11). Therefore, it demonstrates that the carbon in the ore-forming fluids is mainly from the dissolution of carbonate rocks, and which is also about the magmatic rocks.

In general, the δ^{34}S values of sulfides range from –20.2‰ to 1.3‰ with an average of –8.8‰ in the east ore belt. The average δ^{34}S values of galena in the Hexi ore block is –14.4‰; that of sphalerite in the Yanzidong ore block is –10.6‰; that of sphalerite in the Huishan ore block is –6.8‰; that of sphalerite and tetrahedrite in the Heishan ore block is –2.1‰; that of celestine in the Hexi ore block is 17.6‰, and that of celestine in the Yanzidong ore block is 18.9‰, respectively (Table 3; Fig. 12). The predominant negative values of δ^{34}S in the east ore belt indicate that mineralization is linked to biological reduction sulfur. The δ^{34}S values of celestine range from 17.1‰ to 19.4‰ (Table 3), close to the value of total sulfur isotopic composition of ore-forming fluid and that of seawater sulfate. Generally, organic thermos-chemical reduction requires the ore-forming temperature higher than 80°C; the inorganic thermos-chemical reduction demands that higher than 250°C. The ^{34}S values of sulfate would be reduced by 10‰ to 15 ‰ at 100°C to 150°C by thermochemical sulfate reduction (Machel et al., 1995; Ohmoto and Goldhaber, 1997). In this study, the ore-forming temperature of east ore belt is of 150°C, i.e., 2‰ to 10‰ δ^{34}S values can be acquired via organic TSR in our study area. In short, we can infer that biological reduction sulfur participates in the mineralization. In the west ore belt, the δ^{34}S values concentrate between 4‰ and 8‰ (Table 3; Fig. 12), indicating that the deposit has uniform sulfur source. Previous researches showed that the sulfur was from organic thermochemical sulfate reduction of marine sulfate in the Yunlong formation and the decomposition of sulfur-bearing organic matters (Wang Xiaohu et al., 2012). From existing data, the S isotope values of sphalerite is higher than that of galena, which indicate it reached isotope exchange equilibrium between sphalerite and galena. Thus, the formula of paragenetic mineral pairs $1000\ln\alpha=0.78/T^2\times10^6$ (Czamanske and Rye, 1974) can be used to calculate the ore-forming temperature, yielding 228.5°C to 245.5°C and 322°C to 336.3°C, respectively.

In absence of external strontium contamination, the

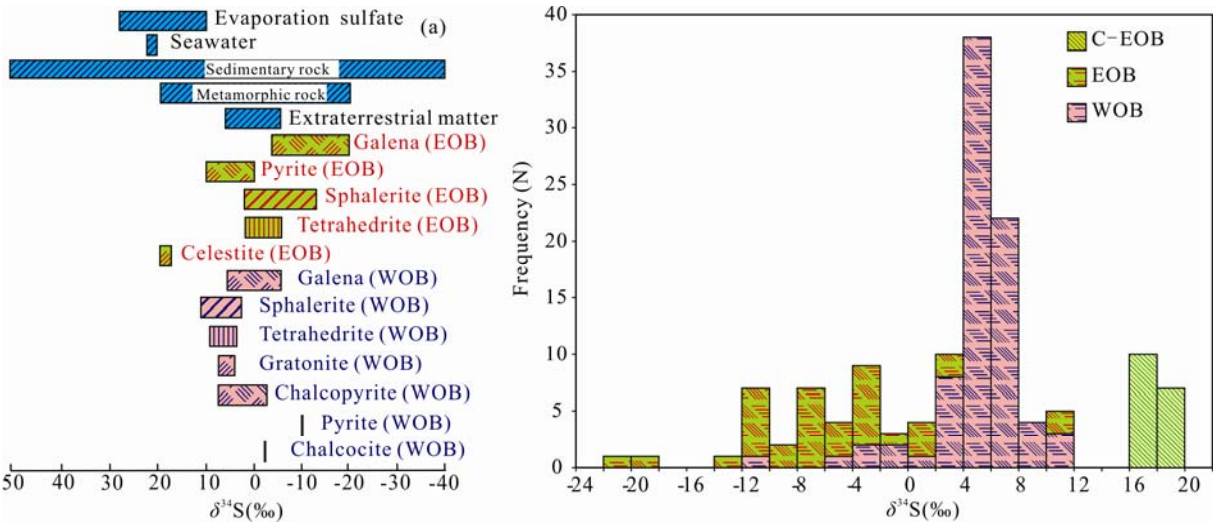

Fig. 12. Sulfur values of sulfide and sulfate from the Baiyangping Pb-Zn polymetallic ore concentration area and important geological reservoirs.
EOB, East ore belt; WOB, West ore belt; C-EOB, Celestite of east ore belt. Data are listed in Table 3.

value of $^{87}Sr/^{86}Sr$ of strontium-rich gangue minerals in ore veins may indicate its source of ore-forming minerals. Ca^{2+} in calcite lattice can be replaced by Sr but not Rb, which makes the Rb/Sr ratio low. In addition, the initial Sr isotopic composition is not significantly affected by the decay of Rb to Sr. Thus, $^{87}Sr/^{86}Sr$ of calcite may be considered as initial Sr isotope composition of ore-forming fluids from calcite precipitation (Hecht et al., 1999; Li et al., 2007). In this study, the Sr isotope ratios of calcite and celestite are between 0.707669 and 0.710115 with the average of 0.709320, in range of crustal source and close to the modeled evolution line of Sr isotope composition in the upper mantle as well as that of recrystallized limestone (0.70977; Ye Qingtong et al., 1992). Therefore, the Sr bearing minerals are most likely from strata and basement.

In comparision of Pb isotope data to that of the whole rock in the adjacent strata (Chen Shifang et al., 1991; Wang Feng, 2004; Song Yucai, 2009) (Table 3), it shows that the Pb isotope values from the Baiyangping district is close to the whole rock Pb isotope value from the adjacent strata (Wang et al., 2015; Wang Xiaohu et al., 2016). The Lanping Basin is composed of Proterozoic schist, migmatite, and granite; Cambrian schist and dolomite; Permian tuff, limestone, basalt, and keratophyre; Triassic rhyolite, basalt, and limestone; Jurassic sandstones; and Tertiary sandstones (Chen Shifang et al., 1991) without Mesozoic - Cenozoic magmatic rocks (YBGMR, 1974, 1984). The basement rocks of the Lanping Basin are made of Permian and Triassic sequences. And more, the elements of Ti, Co, Cu, Zn, As and Sb all have the largest average values in the ultrabasic rocks and basic rocks of the middle region of "Sanjiang" area (Pan Guitang et al., 2003). Therefore, it reasonably infers that the metals of the Baiyangping district are likely derived from both the sedimentary cover and the basement rocks.

6.4 The reason for metallogenic differences of eastern and western ore belts

The east and west ore belts share the same metallogenic age and are only a few kilometers apart. However, the ore-forming elements in the west ore belt are mainly Pb, Zn, Cu, Ag, and Co but dominantly Pb, Zn, Ag, and Sr in the east ore belt. The Co and Ni are found in the western ore belt, but not found in the eastern ore belt. In Fig. 12, the S isotopic compositions of the east and west ore belts are different: It is more heavy sulfur enriched in the west ore belt. It was suggested that the sulfur in the west ore belt is derived from the thermochemical reduction of organic matters of sulfates and the thermal decomposition of organic matters (Wang Xiaohu et al., 2011a). The sulfur isotopic composition of the east ore belt shows a multisource of sulfur. The difference between the east and the west ore belts could be caused by the superimposed mineralization (Wang et al., 2015) and different material influxes: Previous researches proposed that the eastern Lanping Basin could be Jinshajiang, i.e., Yangtze sourced while the western basin more Lancangjiang, i.e., Gondwana sourced (Pan Guitang et al., 2003). Considering the Mesozoic and Cenozoic evolution of the Lanping Basin: The structure of the basin is characterized by two depressions on the sides and a foreland uplift in the middle (Li Xingzhen et al., 1999), which hindered the exchange of materials on the east and west sides of the basin, resulted in the asymmetry of elements in both sides of strata. During ore-forming stage, the east and west

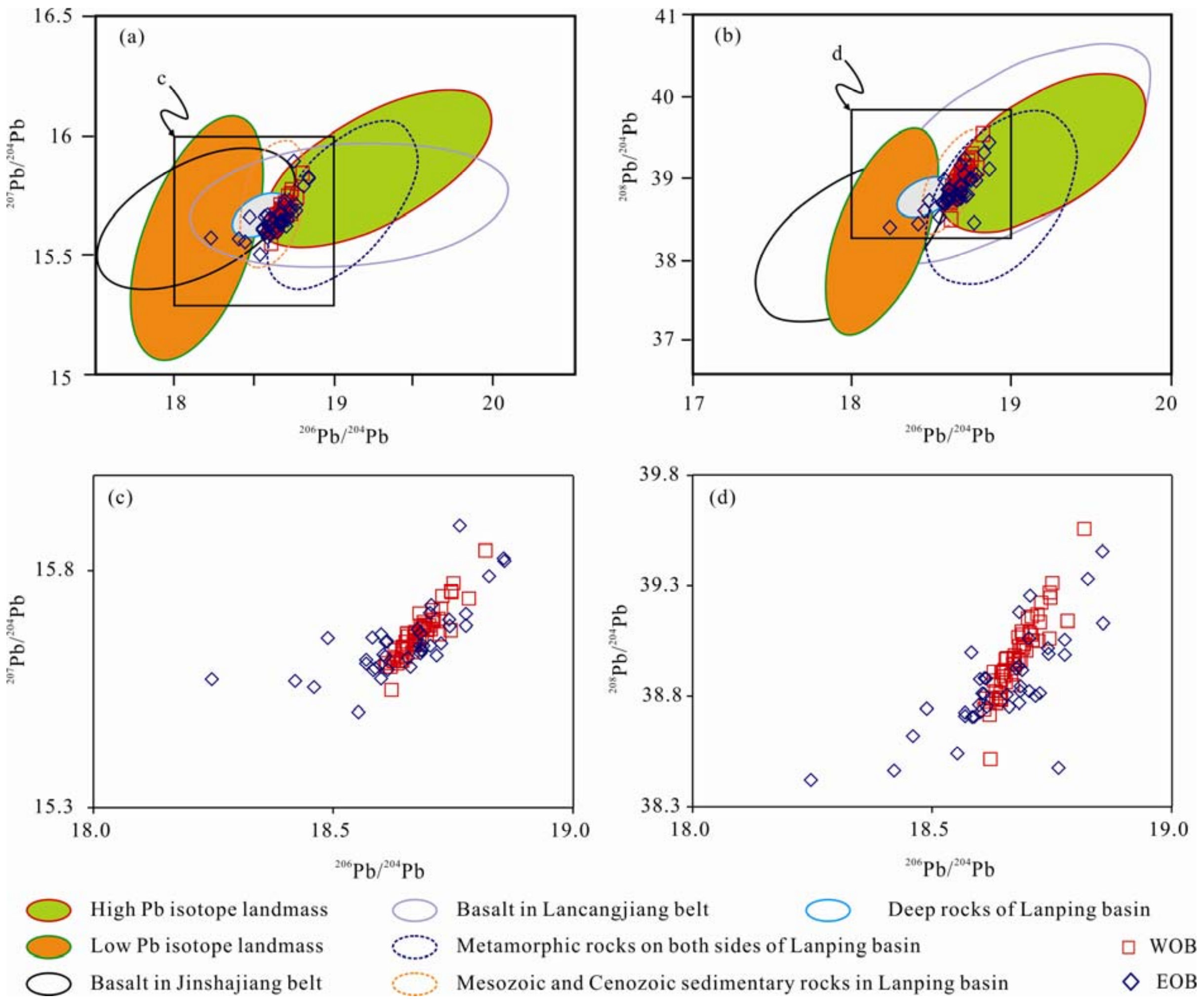

Fig. 13. Comparison chart of Pb isotope compositions from the Baiyangping ore concentration area and possible source end members.
Base map from (Pan Guitang et al., 2003). Data are listed in Table 3.

thrust systems plus the uplift of basin ridge block the transportation of the ore-forming materials between the east and west ore belts, yielding the difference between the east and west belts (Fig. 13). Although the metallogenic metals are from the strata and basement, the metallogenic elements are different.

7 Conclusions

Both ore belts had a homogeneous carbon sources; the carbon in hydrothermal calcite is derived from the dissolution of carbonate rock strata; the ore-forming fluids are from the formation water and precipitate water.

The sulfur was from organic thermal chemical sulfate reduction and biogenic sulfur was involved in metallogenesis; the metal mineralization material is from sedimentary strata and basement. The difference in metallogenic elements between the eastern and western metallogenic belts is produced from different material sources and superimposed mineralization.

The east and the west belts share the same mineralization ages from the Pb-Zn data; the activation of the thrust systems is likely coeval between Eocene and Oligocene.

Acknowledgements

This work is granted by the National Natural Science Foundation of China (grants No. 41302067, 41472067 and 41403043), the Fundamental Research Funds of Chinese Academy of Geological Sciences (grant No. YYWF201614 and 09 program of Institute of Geomechanics), IGCP/SIDA–600, and China Geological Survey (grant No. DD20160053). We thank Dr. Zhang Qing for improving the manuscript.

Manuscript received Feb. 15, 2017
accepted Aug. 10, 2017

edited by Hao Qingqing

References

YBGMR, 1974. *Geological map (scale 1/200,000) with geological report of Lanping (block G–47–X VI)*.

YBGMR, 1984. *Geological map (scale 1/200,000) with geological report of Weixi (block G–47–X)*.

YBGMR, 1995. *Geological map (scale 1/50,000) with geological report of Weixi (block G–47–43–D)*.

Chen Kaixu, 2006. *The forming mechanism of copper–silver polymetallic ore concentration area in the north of Lanping forelanbasin in Yunnan province*. Wuhan: China University of Geosciences (Ph. D thesis): 1–160 (in Chinese with English abstract).

Chen Kaixu, He Longqing, Wei Junqi, Yang Aiping, Yang Weiguang and Huang Huilan, 2004a. Preliminary study on the characteristics of ore minerals and the occurrence states of silver and cobalt in the Baiyangping ore–concentrated field, Yunnan Province. *Acta Mineralogica Sinica,* 24: 61–67 (in Chinese with English abstract).

Chen Kaixu, He Longqing, Yang Zhenqiang, Wei Junqi and Yang Aiping, 2000. Oxygen and carbon isotope geochemistry in Sanshan–Baiyangping copper–silver polymetallogenic enrichment district, Lanping, Yunnan. *Geology and Mineral Resources of South China,* 4: 1–8 (in Chinese with English abstract).

Chen Kaixu, Yao Shuzhen, He Longqing, Yang Aiping, Yang Weiguang and Huang Huilan, 2004b. Ore–forming fluid in Baiyangping silver–polymetallic mineralization concentration field in Lanping, Yunnan province. *Geological Science and Technology Information,* 23: 45–50 (in Chinese with English abstract).

Chen Shifang, Liu Yilai, Bao Yuxiu, Meng Jizhou and Zou Yongbin, 1991. Research into metallogenic law, ore deposit types of Deqin–Xiaguang lead–zinc ore zone. *Yunnan Geology,* 10: 119–144 (in Chinese).

Clark, I.D., and Fritz, P., 1997. *Environmental isotopes in hydrogeology*. New York: Lewis Publishers, 1–328.

Czamanske, G.K., and Rye, R.O., 1974. Experimentally determined sulfur isotope fractionations between sphalerite and galena in the temperature range 600 degrees to 275 degrees C. *Economic Geology,* 69: 17–25.

Deng, J., Wang, Q., Li, G., Li, C., and Wang, C., 2014a, Tethys tectonic evolution and its bearing on the distribution of important mineral deposits in the Sanjiang region, SW China. *Gondwana Research*, 26: 419–437.

Deng, J., Wang, Q. F., Li, G. J., and Santosh, M., 2014b, Cenozoic tectono-magmatic and metallogenic processes in the Sanjiang region, southwestern China. *Earth-Science Reviews*, 138: 268–299.

Deng, J., Wang, C., Bagas, L., Selvaraja, V., Jeon, H., Wu, B., and Yang, L., 2016, Insights into ore genesis of the Jinding Zn–Pb deposit, Yunnan Province, China: Evidence from Zn and in-situ S isotopes. *Ore Geology Reviews*, 90: 943–957.

Deng Shuangling, 2011. Geological feature and genesis for the Liziping Pb–Zn ore block. *Acta Geologica Sichuan,* 31: 323–325+328 (in Chinese with English abstract).

Dong Fangliu, Mo Xuanxue, Hou Zengqian, Wang Yong, Bi Xianmei and Zhou Su, 2005. Ar–Ar ages of Himalayan alkaline rocks in Lanping Basin, Yunnan province, and their geological implication. *Acta Petrologica et Mineralogica,* 24: 103–109 (in Chinese with English abstract).

Fan Weiming, 1992. On Lanpin–Siman Diwa Basin and magmati rocks in its neigbouring regions, western Yunnan. *Geotectonica et Metallogenia,* 16: 83–84 (in Chinese).

Feng Caixia, Bi Xianwu, Hu Ruizhong, Liu Shen, Wu Liyan, Tang Yongyong and Zou Zhichao, 2011. Study on paragenesis –separation mechanism and source of ore–forming element in the Baiyangping Cu–Pb–Zn–Ag polymetallic ore deposit, Lanping Basin, southwestern China. *Acta Petrologica Sinica,* 27: 2609–2624 (in Chinese with English abstract).

Feng C.X., Bi X.W., Liu S., and Hu R.Z., 2014. Fluid inclusion, rare earth element geochemistry, and isotopic characteristics of the eastern ore zone of the Baiyangping polymetallic Ore district, northwestern Yunnan Province, China. *Journal of Asian Earth Sciences,* 85: 140–153.

Fu Xiugen, 2005. Evolution of Lanping Basin and formation of relevant metal deposits. *Journal of Earth Sciences and Environment,* 27: 26–32 (in Chinese with English abstract).

Gong Xuejing, Yang Zhusen, Meng Xiangjin, Pan Xiaofei, Wang Qian and Zhang Lejun, 2017. Late Paleozoic to Mesozoic Intrusions Distribution in the North Sanjiang Orogenic Belt, Southwest China: Evidence from Zircon U–Pb Dating and Geochemistry. *Acta Geologica Sinica* (English Edition), 91: 898–946.

He Longqing, Chen Kaixu, Wei Junqi and Yu Fengming, 2005. Geologicl and geochemical characteristics and genesis of ore deposits in eastern ore belt of Baiyangping area, Yunnan Province. *Mineral Deposits,* 24: 61–70 (in Chinese with English abstract).

He Longqing, Chen Kaixu, Yu Fengming and Wei Junqi, 2004. Mappe tectonics and their ore–controlling of Lanping Basin in Yunnan province. *Geology and Prospecting,* 40: 7–12 (in Chinese with English abstract).

He Longqing, Ji Wei, Chen Kaixu, Yu Fengming, Wei Junqi, Yang Aiping and Yang Weiguang, 2007. Ore–controlled effect of nappe structure in the east ore zone of the Baiyangping area, Lanping Basin, Yunnan. *Journal of Geomechanics,* 13: 110–118 (in Chinese with English abstract).

He L.Q., Song Y.C., Chen K.X., Hou Z.Q., Yu F.M., Yang Z.S., Wei J.Q., Li Z., and Liu Y.C., 2009. Thrust–controlled, sediment–hosted, Himalayan Zn–Pb–Cu–Ag deposits in the Lanping foreland fold belt, eastern margin of Tibetan Plateau. *Ore Geology Reviews,* 36: 106–132.

He Mingqin, Liu Jiajun, Li Chaoyang, Li Zhiming and Liu Yuping, 2004b. *Fluid mineralozation mechanism of a large copper–lead–zinc ore–concentrated area in Lanping Basin–Taking Baiyangping copper–cobalt polymetallic area as the example*. Beijing: Geological Publishing House, 1–117 (in Chinese).

He Mingqin, Liu Jiajun, Li Chaoyang, Li Zhiming, Liu Yuping, Yang Aiping and San Haiqing, 2004a. Ar–Ar Dating of ore quartz from the Baiyangping Cu–Co polymetallic mineralized concentration area, Lanping, Yunnan. *Chinese Journal of Geology,* 41: 688–693 (in Chinese with English abstract).

He Mingyou, Bai Xianzhou, Zhang Chengyuan and Tang Yao, 2009. The ore–forming fluid geochemistry and its geological significance of Baiyangping orefield, Yunnan Province. *Acta Mineralogica Sinica,* S1: 213–214 (in Chinese with English abstract).

Hecht, L., Freiberger, R., Gilg, H.A., Grundmann, G., and

Kostitsyn, Y.A., 1999. Rare earth element and isotope (C, O, Sr) characteristics of hydrothermal carbonates. genetic implications for dolomite–hosted talc mineralization at Göpfersgrün (Fichtelgebirge, Germany). *Chemical Geology,* 155: 115–130.

Hou Zengqian, Hou Liwei, Ye Qingtong, Liu Fulu and Tang Guoguang, 1995. *Tectono–magmatic evolution and volcanogenic massive sulphide deposits in the Yidun island–arc, Sanjiang Region, China.* Beijing: Earthquake Publishing House, 1–218 (in Chinese).

Hou Zengqian, Song Yucai, Li Zheng, Wang Zhaolin, Yang Zhiming, Yang Zhusen, Liu Yingchao, Tian Shihong, He Longqing, Chen Kaixu, Wang Fuchun, Zhao Chenxiang, Xue Wanwen and Lv Haifeng, 2008. Thrust–controlled, sediments –hosted Pb–Zn–Ag–Cu deposits in eastern and northern margins of Tibetan orogenic belt. Geological features and tectonic model. *Mineral Deposits,* 27: 123–144 (in Chinese with English abstract).

Hou, Z.Q., and Zhang H.R., 2015. Geodynamics and metallogeny of the eastern Tethyan metallogenic domain. *Ore Geology Reviews,* 70: 346–384.

Kong Yunli and Qi Linkun, 2009. The genesis of Liziping Pb–Zn deposit of Zhongpai in Lanping, Yunnan. *Yunnan Geology*, 28: 275–279.

Leach, D.L., Sangster, D.L., Kelly, K.D., Large, R.R., Garven, G., Allen, C.R., Gutzmer, J., and Walter, S., 2005. Sediment–hosted lead–zinc deposits. a global perspective. In: Hedenquist, J.,W., Thompson, J.F.H., Goldfarb, R.J., and Richards, J.P. (eds.), SEG 100th Anniversary Special Publication: 561–607.

Li Mei, 2004. Petrological characteristics of volcanic rocks in the Shiden–Tu'e area, Lanping County, Yunnan. *Geology in China,* 31: 64–69 (in Chinese with English abstract).

Li, W., Huang, Z., and Yin, M., 2007. Isotope geochemistry of the Huize Zn–Pb ore field, Yunnan Province, Southwestern China: Implication for the sources of ore fluid and metals. *Geochemical Journal,* 41: 65–81.

Li Xingzhen, Liu Wenju, Wang Yizhao and Zhu Qinwen, 1999. *The tectonic evolution and metallogenesis in the Tethys of the Nujiang–Lancangjiang–Jinshajiang area, southwestern China.* Beijing: Geological Publishing House, 1–276 (in Chinese with English abstract).

Li Yalin, Wang Chengshan, Yi Haisheng, Liu Zhifei and Li Yong, 2006. Cenozoic thrust system and uplifting of the Tanggula Mountain, Northern Tibet. *Acta Geologica Sinica,* 80: 1118–1131 (in Chinese with English abstract).

Li Yike, Wang Anjian, Cao Dianhua and Guan Ye, 2016. The electrical conductivity structure of the Lanping–Simao basin and its implications for mineralization. *Acta Geologica Sinica* (English Edition), 90: 1055–1056.

Li Zhiming, Liu Jiajun, Qin Jianzhong, Liao Zongting, He Mingqin and Liu Yuping, 2005. Ore–forming material sources of the Baiyangping copper–cobalt–silver polymetallic deposit in Lanping Basin, western Yunnan. *Geology and Prospecting,* 41: 1–6 (in Chinese with English abstract).

Li Zhiming, Liu Jiajun, Qin Jianzhong, Liao Zongting and Zhang Changjiang, 2004. C, O and H isotopic compositions of polymetallic deposits in Lanping Basin, western Yunnan province and their geological significance. *Journal of Jilin University* (Earth Science Edition), 34: 360–366 (in Chinese with English abstract).

Liu Jiajun, He Mingqin, Li Zhiming, Liu Yuping, Li Chaoyang, Zhang Qian, Yang Weiguang and Yang Aiping, 2004. Oxygen and carbon isotope geochemistry of Baiyangping silver–copper polymetallic ore concentration area in Lanping Basin of Yunnan province and its significance. *Mineral Deposits,* 23: 1–10 (in Chinese with English abstract).

Liu Jiajun, Zhai Degao, Li Zhiming, He Mingqin, Liu Yuping and Li Chaoyang, 2010. Occurrence of Ag, Co, Bi and Ni elements and its genetic significance in the Baiyangping silver –copper polymetallogenic concentrartion area, Lanping Basin, southwestern China. *Acta Petrologica Sinica,* 26: 1646–1660 (in Chinese with English abstract).

Liu Zengqian, Li Xingzhen, Ye Qingtong, Luo Jianning, Shen Ganfu, Mo Xuanxue, Chen Fuzhong, Chen Bingwei, Yang Yueqing, Lv Boxi, Chen Jishen, Pan Guitang, Jia Baojiang, Hu Yunzhong and Zheng Lailin, 1993. *Division of tectono–magmatic zones and the distribution of deposits in the Sanjiang area (Nujiang–Lancangjiang–Jinshajiang area).* Beijing: Geological Publishing House, 1–246 (in Chinese with English abstract).

Liu Zengqian, Pan Guitang and Zheng Haixiang, 1983. *A preliminary study on the north boundary and the evolution of Gondwana and Tethys in light of the new data on Qinghai–Xizang (Tibet) Plateau. Committee of Geological Memoirs of Qinghai–Xizang, Geological Memoirs of Qinghai–Xizang Plateau (12).* Beijing: Geological Publishing House, 11–24 (in Chinese with English abstract).

Machel, H.G., Krouse, H.R., and Sassen, R., 1995. Products and distinguishing criteria of bacterial and thermochemical sulfate reduction. *Applied Geochemistry,* 10: 373–89.

Mo Xuanxue, Lu Fengxiang, Shen Shangyue, Zhu Qinwen, Hou Zengqian, Yang Kaihui, Deng Jinfu, Liu Xiangpin and He Changxiang, 1993. *Sanjiang Tethys volcanism and related mineralization.* Beijing: Geological Publishing House, 1–267 (in Chinese with English abstract).

Mou Chuanlong, Wang Jian, Yu Qian and Zhang Lisheng, 1999. The evolution of the sedimentary basin in Lanping area during Mesozoic–Cenozoic. *Journal of Mineralogy and Petrology,* 19: 30–36 (in Chinese with English abstract).

Ohmoto, H., 1972. Systematics of sulfur and carbon isotopes in hydrothermal ore deposits. *Economic Geology,* 67.

Ohmoto, H., and Goldhaber, M., 1997. Sulfur and carbon isotopes. In: Barnes, H., L. (ed.), *Geochemistry of hydrothermal ore deposits (3rd edition).* New York: Wiley–Inter science, 509–567.

Pan Guitang, Xu Qiang, Hou Zengqian, Wang Liquan, Du Dexun, Mo Xuanxue, Li Dingmou, Wang Mingjie, Li Xingzhen, Jiang Xinsheng and Hu Yunzhong, 2003. *Archipelagic orogenesis, metallogenic systems and assessment of the mineral resources along the Nujiang–Lancangjiang–Jinshajiang area in southwestern China.* Beijing: Geological Publishing House, 1–420 (in Chinese with English abstract).

Qian Xianggui and Lv Boxi, 2000. The petrographic features and genesis of Cenozoic alkali volcanic rocks in the Three–rive area, west Yunnan. *Yunnan Geology,* 19: 152–170 (in Chinese with English abstract).

Qin Gongjiong and Zhu Shangqing, 1991. Genetic model and prospecting prediction of Jinding lead–zinc ore deposit. *Yunnan Geology,* 10: 145–190 (in Chinese with English abstract).

Que Meiying, Chen Dunmo, Zhang Lisheng, Xia Wenjie and Zhu Chuangye, 1998. *Copper deposits in Lanping–Simao Basins*. Beijing: Geological Publishing House, 1–109 (in Chinese with English abstract).

Rajabi, A., Rastad, E., and Canet, C., 2012. Metallogeny of Cretaceous carbonate–hosted Zn–Pb deposits of Iran. geotectonic setting and data intergration for future mineral exploration. *International Geology Review,* 54: 1649–1672.

Rollinson, H. R., 1993. *Using Geochemical Data: Evaluation, Presentation, Interpretation*. New York, John Wiley and Sons. 1–352.

Shao Zhaogang, Meng Xiangang, Feng Xiangyang and Zhu Dagang, 2002. Analysis on the ore–forming geodynamics of the Baiyangping ore–concentrated field, Yunnan province. *Acta Geoscientica Sinica,* 23: 201–206 (in Chinese with English abstract).

Shao Zhaogang, Meng Xiangang, Feng Xiangyang and Zhu Dagang, 2003. Tectonic characteristics of the Baiyangping–Huachangshan ore belt, Yunnan province and its ore–controlling effect. *Journal of Geomechanics,* 9: 246–253 (in Chinese with English abstract).

Song Yucai, 2009. *Characteristics and genetic model of sediment–hosted base metal deposits in Sanjiang area, Southwest China,* Beijing: Chinese Academy of Geological Sciences (Postdoctoral report): 1–118 (in Chinese with English abstract).

Spurlin, M.S., Yin, A., Horton, B.K., Zhou, J.Y., and Wang, J.H., 2005. Structural evolution of the Yushu–Nangqian region and its relationship to syncollisional igneous activity, eastcentral Tibet. *GSA Bulletin,* 117: 1293–1317.

Tan Fuwen, Xu Xiaosong, Yin Fuguang and Li Xingzhen, 1999. Upper Carboniferous sediments in the Simao region, Yunnan and their tectonic settings. *Sedimentary Facies and Palaeogeography,* 19: 26–34 (in Chinese with English abstract).

Tao Xiaofeng, Zhu Lidong, Liu Dengzhong, Wang Guozhi and Li Youguo, 2002. The formation and evolution of the Lanping Basin in western Yunnan. *Journal of Chengdu University of Technology,* 29: 521–525 (in Chinese with English abstract).

Teng Yanguo, Liu Jiaduo, Zhang Chengjiang, Ni Shijun and Peng Xiuhong, 2001. Trace element characteristics of magmatic rocks in the Lanping Basin and its neighboring areas. *Journal of Chengdu University of Technology,* 28: 40–44(in Chinese with English abstract).

Tian Hongliang, 1997. Geological features of Baiyangping copper–silver polymetallic deposit, Lanping. *Yunnan Geology,* 16: 105–108 (in Chinese).

Wang, C., Deng, J., Carranza, E. J. M., and Santosh, M., 2014, Tin metallogenesis associated with granitoids in the southwestern Sanjiang Tethyan Domain: Nature, deposit types, and tectonic setting. *Gondwana Research*, 26: 576–593.

Wang Feng, 2004. *Geochemical mechanisms of Baiyangping silver polymetallic deposits formation, Yunnan,* Chengdu: Chengdu University of Technology (Ph. D thesis): 1–77 (in Chinese with English abstract).

Wang Feng and He Mingyou, 2003. Lead and sulfur isotopic tracing of the ore–formin material from the Baiyangping copper–silver polymetallic deposit in Lanping, Yunnan. *Sedimentary Geology and Tethys Geology,* 23: 82–85 (in Chinese with English abstract).

Wang, J.H., Yin, A., Harrison, T.M., Grove, M., Zhang, Y.Q., and Xie, G.H., 2001. A tectonic model for Cenozoic igneous activites in the eastern Indo–Asian collision zone. *Earth and Planetary Science Letters,* 188: 123–133.

Wang Xiaohu, Hou Zengqian, Song Yucai, Wang Guanghui, Zhang Hongrui, Zhang Chong, Zhuang Tianming, Wang Zhe and Zhang Tianfu, 2012. Baiyangping Pb–Zn–Cu–Ag polymetallic deposit in Lanping Basin: a discussion on characteristics and source of ore–forming fluids and source of metallogenic materials. *Earth Science–Journal of China University of Geosciences,* 37: 1015–1028 (in Chinese with English abstract).

Wang Xiaohu, Hou Zengqian, Song Yucai, Yang Tianan and Zhang Hongrui, 2011a. Baiyangping Pb–Zn–Cu–Ag polymetallic deposit in Lanping Basin: metallogenic chronology and region mineralization. *Acta Petrologica Sinica,* 27: 2625–2634 (in Chinese with English abstract).

Wang, X.H., Hou Z.Q., Song, Y.C., and Zhang, H.R., 2015. Geological, fluid inclusion and isotopic studies of the Baiyangping Pb–Zn–Cu–Ag polymetallic deposit, Lanping Basin, Yunnan province, China. *Journal of Asian Earth Sciences,* 111: 853–871.

Wang Xiaohu, Song Yucai, Hou Zengqian, Zhang Hongrui, Wang Zhe, Zhuang Tianming, Zhang Chong and Zhang Tianfu, 2011b. Geological characteristics of the Baiyangping Pb–Zn–Cu–Ag polymetallic deposit in northern Lanping Basin. *Acta Petrologica et Mineralogica,* 30: 507–518 (in Chinese with English abstract).

Wang Xiaohu, Song Yucai, Zhang Hongrui, Liu Yingchao, Pan Xiaofei and Guo Tao, 2016. Geochemical characteristics and metallogenic age of the east ore belt in Baiyangping polymetalloc ore concentration area. *Journal of Geomechanics,* 22: 294–309 (in Chinese with English abstract).

Wang Yanbin, Zeng Pusheng, Li Yanhe and Tian Shihong, 2004. He–Ar isotope composition of Jinding and Baiyangping mineral deposit and its significance. *Journal of Mineralogy and petrology,* 24: 76–80 (in Chinese with English abstract).

Xu Qidong and Zhou Lian, 2004. Ore–forming fluid migration in relation to mineralization zoning in Cu–polymetallic mineralization district of northern Lanping, Yunnan: evidence from lead isotope and mineral chemistry of ores. *Mineral Deposits,* 23: 452–461 (in Chinese with English abstract).

Xu Shihai, Gu Xuexiang, Tang Juxing, Chen Jianping and Dong Shuyi, 2005. Stable isotopic geochemistry of three major types of Cu–Ag polymetallic deposits in the Lanping Basin, Yunnan. *Bulletin of Mineralogy, Petrology and Geochemistry,* 24: 309–316 (in Chinese with English abstract).

Xue Chunji, 2000. *Study on Tertiary metallogenic series of Lanping Basin, Yunnan province,* Beijing: Chinese Academy of Geological Sciences (the Postdoctoral report): 1–47 (in Chinese).

Xue Chunji, Chen Yuchuan, Wang Denghong, Yang Jianming, Yang Weiguang and Zeng Rong, 2003. Geology and isotopic composition of helium, neon, xenon and metallogenic age of the Jinding and Baiyangping ore deposits, northwest Yunnan, China. *Science in China* (Series D)*,* 46: 789–800 (in Chinese with English abstract).

Xue CJ, Zeng R, Liu SW, Chi GX, Qing HR, Chen YC, Yang JM and Wang DH. 2007. Geologic, fluid inclusion and isotopic characteristics of the Jinding Zn–Pb deposit, western Yunnan, South China.: a review. *Ore Geology Reviews,* 31:

337–359.

Xue Chunji, Chen Yuchuan, Yang Jianming, Wang Denghong, Yang Weiguang and Yang Qingbiao, 2002. Jinding Pb–Zn deposit: geology and geochemistry. *Mineral Deposits,* 21: 270–277 (in Chinese with English abstract).

Xue Wei, Xue Chunji, Chi Guoxiang, Shi Haigang, Gao Bingyu and Yang Shoufa., 2010. Study on the fluid inclusions of Baiyangping polymetallic deposit in Lanping Basin, northwestern Yunnan, China. *Acta Petrologica Sinica,* 26: 1773–1784 (in Chinese with English abstract).

Yang Weiguang, 2002. *Geological, geochemical and metallogenic mechanism of the Baiyangping silver–copper polymetallic ore concentration area, Yunnan Province.* Beijing: China University of Geosciences (Ph. D thesis): 1–94 (in Chinese with English abstract).

Yang Weiguang, Yu Xuehui, Li Wenchang, Dong Fangliu and Mo Xuanxue, 2003. The characteristics of metallogenic fluids and metallogenic mechanism in Baiyangping silver and polymetallic mineralization concentration area in Yunnan province. *Geoscience,* 17: 27–33 (in Chinese with English abstract).

Ye Qingtong, Hu Yunzhong and Yang Yueqing, 1992. *Regional geochemical background and gold silver and lead–zinc mineralization in the Nujiang–Lancangjiang–Jinshajiang area.* Beijing: Geological Publishing House, 1–279 (in Chinese with English abstract).

Yu Fengming, He Longqing and Chen Kaixu, 2007. Calcite fabric of tectonite in an ore–controlling fault belt in the Baiyangping east ore district, Yunnan. *Geology in China,* 34: 1130–1140 (in Chinese with English abstract).

Yu Fengming, He Longqing and Chen Kaixu, 2011. Microdeformation characteristics of the tectonite from the Huachangshan fault zone in the Baiyangping ore district, Yunnan Province. *Acta Geoscientica Sinica,* 32: 37–45 (in Chinese with English abstract).

Zeng Pusheng, Hou Zengqian, Gao Yongfeng and Du Andao, 2006. The Himalayan Cu–Mo–Au mineralization in the eastern Indo–Asian collision zone, constraints from Re–Os dating of molybdenite. *Geological Review,* 52: 72–84 (in Chinese with English abstract).

Zeng Rong, 2007. *The Large–scale Fluid Ore–forming Process in the Lanping Basin–Taking the Jinding and Baiyangping deposits as the examples,* Xi'an: Chang'an University (Ph. D thesis): 1–99(in Chinese with English abstract).

Zhang Chengjiang, Ni Shijun, Teng Yanguo, Peng Xiuhong and Liu Jiaduo, 2000. Relationship between Himalayan tectonomagmatic movement and mineralization in Lanping Basin, Yunnan Province. *Journal of Mineralogy and Petrology,* 20: 35–39 (in Chinese with English abstract).

Zhang Hongrui, Hou Zengqian and Yang Zhiming, 2010. Metallogenesis and geodynamics of Tethyan metallogenic domain. A review. *Mineral Deposits,* 29: 113–133 (in Chinese with English abstract).

Zhang, J.R., Wen, H.J., Qiu, Y.Z., Zou Z.C., Du, S.J., and Wu, S.Y., 2015. Spatial–temporal evolution of ore–forming fluids and related mineralization in the western Lanping Basin, Yunnan Province, China. *Ore Geology Reviews,* 67: 90–108.

Zhao Haibin, 2006. *Study on the characteristics and metallogenic conditions of copper–polymetallic deposits in middle–northern Lanping Basin, western Yunnan,* Beijing: China University of Geosciences (Ph. D thesis): 1–123 (in Chinese with English abstract).

Zhu Dagang, Meng Xiangang, Feng Xianyang, Yang Weiguang, Shao Zhaogang, Yang Aiping, Zhou Wenguang, Yang Meiling and Wang Jianping, 2002. Characteristics of tectonic structures at Baiyangping, Yunnan and Their control over the minerogenesis of polymetal deposit in the ming area. *Geology–Geochemistry,* 30: 28–33 (in Chinese with English abstract).

Zou Zhichao, Hu Ruizhong, Bi Xianwu, Wu Liyan, Feng Caixia and Tang Yongyong, 2012. Study on isotope geochemistry compositions of the Baiyangping silver–copper polymetallc ore deposit area, Yunnan province. *Geochimica,* 41: 515–529 (in Chinese with English abstract).

About the first author

WANG Xiaohu, male, born in 1983 in Sihong County, Jiangsu Province; Ph. D., graduated from Chinese Academy of Geological Sciences, is mainly interested in the study of ore deposits and orefield structure. E-mail: wangzykc@yeah.net.